Tectonostratigraphic analysis of the syn-rift infill in the Drava Basin, southwestern Pannonian Basin System

Rukavina, David; Saftić, Bruno; Matoš, Bojan; Kolenković Močilac, Iva; Premec Fuček, Vlasta; Cvetković, Marko

Tectonostratigraphic analysis of the syn-rift infill in the Drava Basin, southwestern Pannonian Basin System

David Rukavina [a], Bruno Saftić [a,*], Bojan Matoš [a], Iva Kolenković Močilac [a], Vlasta Premec Fuček [b], Marko Cvetković [a]

[a] University of Zagreb, Faculty of Mining, Geology and Petroleum Engineering, Pierottijeva 6, 10000, Zagreb, Croatia
[b] INA, d.d., Lovinčićeva Ulica 4, 10000, Zagreb, Croatia

A B S T R A C T

The Drava Basin in the SW Pannonian Basin System (PBS) was initially formed by passive rifting with accompanying sedimentary infill. Although this has been the subject of much previous work, an account of tectonic control has been lacking. Based on cores, wire logging, and seismic data, the tectonostratigraphic interpretation, depositional systems, and control on depositional systems of the syn-rift infill of the eastern part of the Drava Basin were studied. The rifting phase is characterised by the formation of half-grabens, grabens, a sag, and supradetachment basin structures with structural ramp and structural highs. The syn-rift infill can be divided into second-order tectonostratigraphic sequences corresponding to the early and late rift stages. The second-order sequences are further subdivided into third-order tectonostratigraphic sequences formed in response to higher-order tectonic events associated with local rift migration. In contrast to the early-stage structures, the late-stage rift structures are primarily controlled by extensional detachments that represent parts of the Drava Rift Fault System (DRFS). The early syn-rift is characterised by continental deposition through alluvial fans, fan deltas, and lacustrine environments. The late syn-rift stage is characterised by marine deposition in shallow water, fan deltas, and submarine slope-aprons, with deep marine sedimentation and intense volcanic activity. The ramp, basin slopes, and fault scarp slopes represent the major sediment transport pathways involved in the formation of alluvial fans, fan deltas, or submarine slope-aprons. Basinal sedimentation and major depocenters are located within synforms formed by structural lows in the geometry of extensional detachments. This study gives an example of syn-rift tectonic control for the SW part of the PBS and the influence of detachment geometry on basin fill. We have presented an approach based on 3D seismostratigraphic interpretation of tectonostratigraphic sequences, and the correlation of seismic facies with depositional environments developed in a back-arc setting.

1. Introduction

Tectonic activity plays a key role in the formation of sedimentary successions in most active rift basins during their evolution (Ravnås and Steel, 1998). Sedimentary infill in such a basin records the events of fault activation and changes in their offset rates that control the basin evolution (Matenco and Haq, 2020). When the rate of tectonic subsidence exceeds the cumulative rate of sediment supply and sea-level change, tectonic succession can be observed (Matenco and Haq, 2020). The evolution of sedimentary fill and the resulting basin architecture is characterised by elements controlled by the basement. These include extension magnitude, rift width, size of uplifted structures, erosion, and

transition zones (Gibbs, 1987; Withjack et al., 2002; Hinsken et al., 2007; Milia and Torrente, 2015), which are important for understanding transport and depositional processes (Allen and Hovius, 1998; Andrić et al., 2017; Jia et al., 2019). Rift transport zones (Morley et al., 1990) and fault scarps control the location of the sediment pathways/routing from their sources to depocenters. The influence of tectonic elements on the contained sedimentary systems and depocenters distribution remains a subject of research (Khalil and Mcclay, 2009; Athmer and Luthi, 2011; Zhu et al., 2014; Jia et al., 2019; Muravchik et al., 2020). Structural transfer zones are common sediment-transport pathways (Morley, 1990; Withjack et al., 2002; Athmer and Luthi, 2011; Hou et al., 2012; Zhu et al., 2014; Jia et al., 2019). The different geometry of these zones

---

leads to changes in drainage and pathways. The slope angle of the relay ramp can determine whether sediments are transported directly into the basin or whether ramps can be areas of deposition too (Athmer et al., 2011; Hemelsdaël and Ford, 2016). Understanding of the evolution of the drainage system is crucial for sandstone distribution prediction (Gawthorpe and Leeder, 2000; Feng et al., 2016).

This study extends the knowledge of tectonic controls on basin-fill architecture during passive rifting in border areas (areas where multiple tectonic phases and subsurface deformation are visible due to interaction between regional structural units), such as the Drava Basin in the SW Pannonian Basin System (PBS) near the Dinarides (Figs. 1 and 2) (Royden et al., 1983a, 1983b; Huismans et al., 2001). The Miocene extension, generated by continental collision and subduction in the Carpathian thrust belt, of Adria-Europe related blocks, led to formation of the back-arc Pannonian Basin (Royden et al., 1983a; Windhoffer et al., 2005; Horváth et al., 2006). The sedimentological and stratigraphic records of the syn- and post-rift Lower and Middle Miocene formations in the Croatian PBS have been studied previously (Fig. 3a) at the surface (Pavelić et al., 1998; Pavelić, 2001; Vrsaljko et al., 2005; Zečević et al., 2010; Sremac et al., 2016; Pavelić and Kovačić, 2018) and subsurface (Šimon, 1973; Pavelić, 1987; Tišljar, 1993; Saftić et al., 2003). However, none of these studies analysed the tectonic control on syn-rift basin infill.

Our objectives were to determine the size and type of syn-rift structures, to reconstruct theevolution of basin architecture from the rift onset until the rift cessation, to show the tectonic control on syn-rift deposition, and to define the main sedimentary entry points into the depocenters. This is important for the understanding sandstone distribution and reservoir exploration in the syn-rift infill of the SW part of the PBS. To gain insight into the sedimentary response to the observed syn-rift tectonics, the south-eastern part of the Drava Basin was studied

(Fig. 3). Facies analysis was based on macroscopic, petrographic, and biostratigraphic (planktonic foraminifera) analyses of cores. Tectonostratigraphic interpretation relied primarily on 3D seismic data (Fig. 2), the good quality of which allowed structural interpretation, mapping of sequence boundaries and seismic facies distribution, and analysis of seismic attributes. This allowed a detailed interpretation of the movements in the extensional detachment hanging wall, so that different stratigraphic surfaces of the defined rift sequences can be related to the stages of the basin tectonic evolution. In addition, this study documents extensional structures and differences in their geometry, kinematics, and influence on depositional systems.

2. Geological setting

The Drava Basin is a Neogene-Quaternary sedimentary basin formed in the Early Miocene, as part of the wider PBS that was initiated during the Oligo-Miocene collision between the Adria Microplate and the European foreland, causing a "back-arc" type extension (Royden et al., 1983a; Ratschbacher et al., 1991; Brückl et al., 2010, and references therein). This complex setting resulted in different phases and styles of extension (Tari et al., 1992). The extension was accommodated by low-angle detachment faults and planar normal faults, with different extension rates accommodated by the strike-slip faults.

Structural analysis of Miocene half-grabens of the Great Hungarian Plain (Balázs et al., 2016) have provided important information on rift dynamics in the PBS. The mapped ages of the rift climax provide information on its spatial and temporal migration and the direction of extensional transport direction. At the contact between the Dinarides and PBS (where the Sava and Drava basins are located; Figs. 1 and 2), the direction of the extension was NNE-SSW and was accommodated by mostly asymmetric extensional mechanisms related to extensional
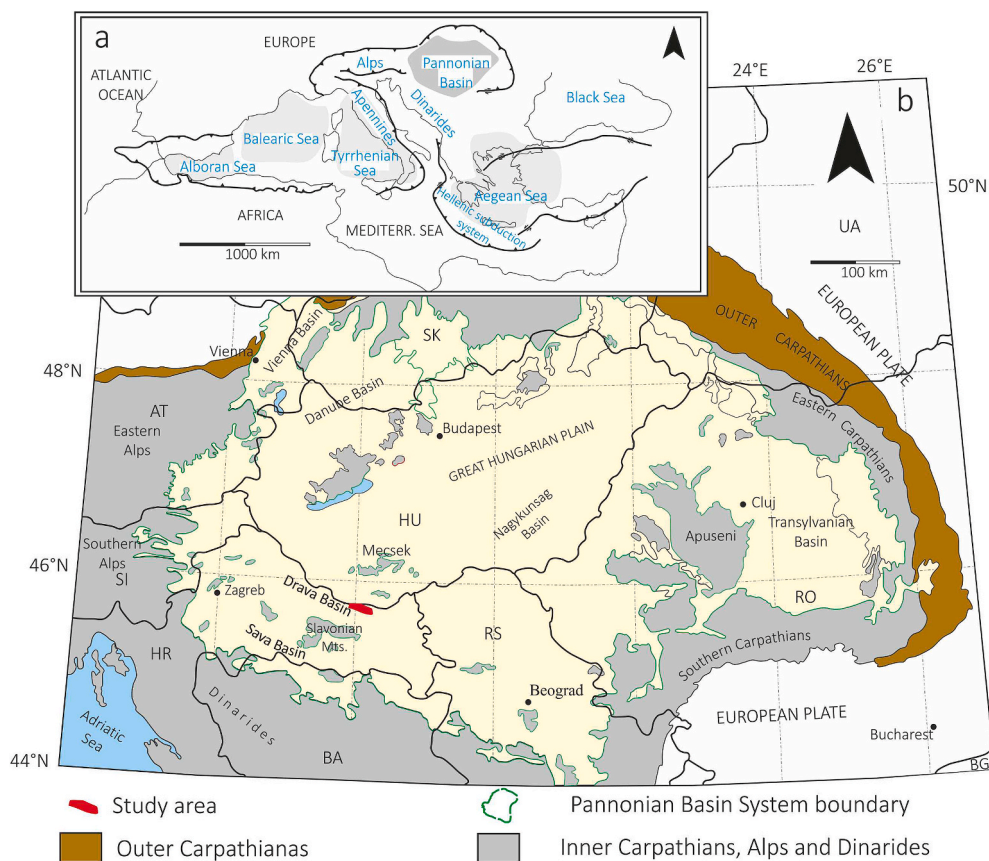

Fig. 1. Tectonic setting of the study area: a) Pannonian Basin System (PBS) and surrounding orogenic belts within the Europe-Mediterranean collision zone (Royden, 1993); b) Regional map of PBS (after Dolton, 2006; Schmid et al., 2008).
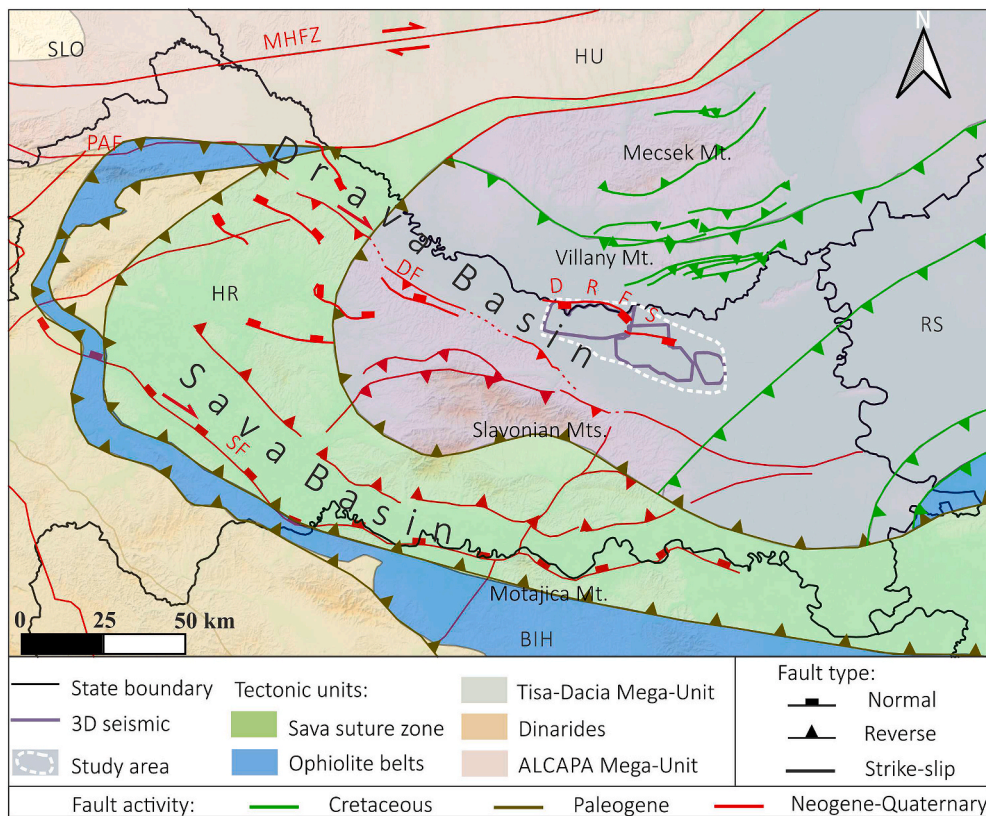
Fig. 2. Map showing regional tectonic units and major neotectonic structures (MHFZ – Mid Hungarian Fault Zone, PAF – Periadriatic Fault, DF – Drava Fault, SF – Sava Fault, DRFS – Drava Rift Fault System). Regional fault systems compiled after Prelogović et al. (1998); Csontos et al. (2002); Bada et al. (2007); Schmid et al. (2008); Ustaszewski et al. (2014a); Matoš et al. (2016). The study area is located within Tisza-Dacia Mega Unit, near the Paleogene (brown) and Late Cretaceous (green) trust sheets and the Sava Suture Zone between the Tisza and Dinarides. Neogene extension was followed by reverse and strike-slip movements that resulted in tectonic uplift of the pre-Neogene basement.

detachment or low-angle faults, favoured by reactivation of inherited low-angle Cretaceous thrust sheets. Exhumation of the footwall of extensional detachments near the Dinarides boundary began in the Oligocene and culminated in the Middle Miocene (Ustaszewski et al., 2010; Stojadinović et al., 2013). In contrast, older works explain the formation of the Drava and Sava Basins by an overall dextral transcurrent displacement along the Drava and Sava faults (DF and SF on Fig. 2.) and rotation of blocks (Jamičić, 1995; Lučić et al., 2001). The direction of tectonic movement has been interpreted as NE, with remaining subsidence within pull-apart basins associated with sinistral faults (Prelogović et al., 1998).

The Drava Basin contains sediments of Neogene-Quaternary age (Fig. 3a; Pavelić and Kovačić, 2018). The oldest Miocene sediments are alluvial and Ottnangian in age (Mandić et al., 2012); they were deposited on the pre-Neogene paleorelief of various Paleozoic and Mesozoic rocks, commonly referred to as the Base Neogene (BNg) surface. Continued rifting led to sedimentation and formation of hydrologically open lake sediments (Pavelić and Kovačić, 2018). The transition from lacustrine to marine deposits on Mt. Papuk (Ćorić et al., 2009) is observed in the lower part of the Nannoplankton Zone NN5, indicating continued sedimentation from the Early to Middle Badenian (Fig. 3a). However, a stratigraphic discontinuity between continental and marine sedimentation is observed at several locations in the Croatian part of the PBS (Mandić et al., 2012). The first tectonostratigraphic study of Miocene sediments in this area (Pavelić, 2001) suggested an unconformable syn-rift/post-rift boundary, the erosional surface formed by the final uplift of footwall blocks. This is consistent with the interpreted regional culmination of extension in the PBS (Horváth et al., 2006; Balázs et al., 2016). The Middle Badenian rocks in that formed in marine offshore environments are largely composed of marls with intercalations of gravity-flow deposits and nearshore sediments represented by shallow-water calcarenites and conglomerates (Pavelić et al., 1998; Pavelić and Kovačić, 2018). Contemporaneous volcanic and pyroclastic rock formations resulted from increased volcanic activity (Pavelić, 2001;

Pavelić and Kovačić, 2018) (Fig. 3a). Late Badenian and Sarmatian ages were characterised by continued marine environments represented by basal conglomerates above the syn-rift/post-rift boundary, algal and reef limestones, biocalcarenites, and marls (Vrsaljko et al., 2005; Vrsaljko et al., 2006; Pavelić and Kovačić, 2018). The total thickness of the Lower and Middle Miocene sediments in the eastern part of the Drava Basin locally exceeds 1 km (3 b) (Saftić et al., 2003).

Following the episodic Sarmatian compression event (e.g. Horváth, 1995), Late Miocene and Early Pliocene tectonics in the Drava Basin was driven by extension associated with thermal subsidence, which was replaced by regional Late Pliocene-Quaternary compression/transpression with different stress orientations (e.g., Müller et al., 1992; Prelogović et al., 1998; Saftić et al., 2003; Bada et al., 2007; Matoš, 2014; Ustaszewski et al., 2014; Pavelić and Kovačić, 2018). The latter stresses were trigered by the northward movement of the Adria Microplate during the Pliocene and Quaternary, which changed the regional stress orientation, resulting in predominantly horizontal shortening (Grenerczy et al., 2005, and references therein). As a result, the entire PBS was reactivated with compressional-transpressional tectonic inversion of inherited fault structures (Bada et al., 2007; Ustaszewski et al., 2014, and references therein). Kilometre-scale folds and pop-up structures (the Slavonian Mountains) were observed (Fig. 2) (e.g. Tomljenović and Csontos, 2001; Bada et al., 2007; Matoš, 2014). During the Late Miocene, the Drava Basin was filled with sediments from Lake Pannon (Saftić et al., 2003, and references therein). This sedimentation was characterised by clastic successions (Pavelić and Kovačić, 2018) that trended toward deltaic progradation (Fig. 3a) with sediment transport from the Eastern Alps (Magyar et al., 1999). These Upper Miocene rocks comprise most of the basin fill and reach up to 5 km in thickness (Saftić et al., 2003). In the latest tectonic phase, Pliocene and Quaternary sedimentation followed the above-mentioned basin inversion (Velić et al., 2011; Cvetković, 2013; Mandić et al., 2015). These depositional sequences are freshwater sediments of Lake Slavonia, formed from the remains of the large brackish Lake Pannon (Harzhauser
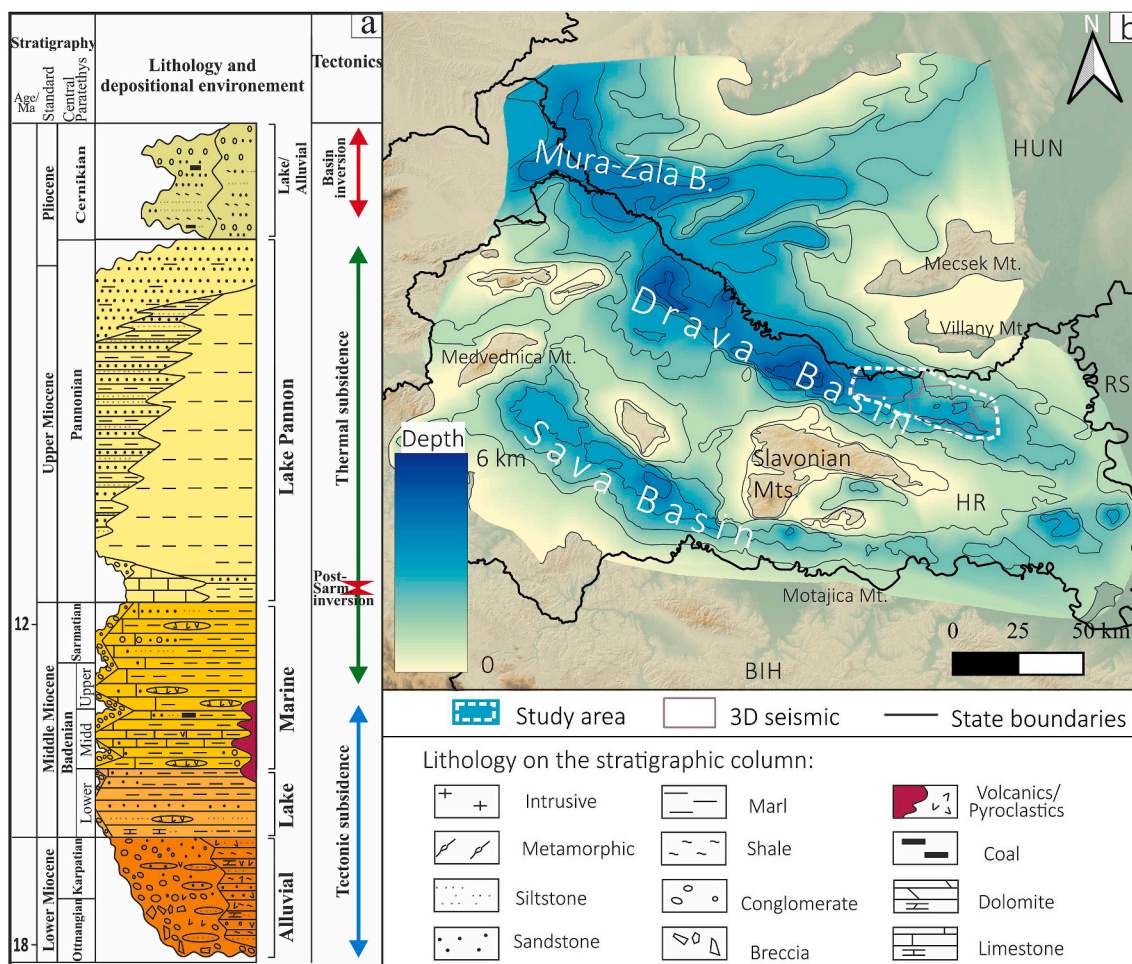
Fig. 3. a) Stratigraphy, lithology, and depositional environments of the Neogene of the North Croatian Basin (Pavelić and Kovačić, 2018), with planktonic fora-minifera and calcareous nanoplankton after (Piller et al., 2007). Note the diverse lithologies during the syn-rift phase and the normal regression of Lake Pannon in the post-rift phase; b) Map showing the depth and total thickness of the Neogene infill of the SW part of the Pannonian Basin (after Saftić et al., 2003; Bali et al., 2012; Cvetković et al., 2019).

and Mandic, 2008).

3. Data and methods

Cores, well logs, and seismic data were used for the study. Tectonostratigraphy was interpreted from 3D seismic data for an area of 538 km^2 near the Croatian–Hungarian border (Figs. 2 and 3b). The Schlumberger Petrel E&P Software Platform was used for structural and stratigraphic interpretation of the seismic and well data. Cores were taken from the selected interval in eight of the 17 existing wells in the area. Core samples were examined macroscopically and microscopically (thin sections) to understand the lithology and sedimentary features.

Seismic reflection characteristics were used in combination with borehole data to determine the relationship between seismic facies and facies association (Figs. 4 and 5) and types of syn-rift structures (Figs. 6 and 7) and sequence boundaries. Sequence stratigraphical interpretation was based on recognition of the sequence boundary characteristics, according to Embry (1995). All boundaries are primarily delineated by tectonic activity (Figs. 8–11). The higher-order cyclicity of the sequences visible in the seismic data is related to the activity of individual faults and is interpreted in terms of transgressive-regressive cycles as defined by Balázs et al. (2016) and Andrić et al. (2017). Based on the analysis of core samples, seismic facies, and seismic attributes in the main depocenters (Figs. 12 and 13), different depositional environments were determined (Fig. 5). Depositional features within the mapped

sequences were examined in detail using a multi-attribute analysis of seismic volume (Root Mean Square amplitude and Variance) in the western part of the study area, where the best 3D data set was available. Tectonic control on the internal structure of the sequence was also interpreted.

4. Results

4.1. Facies and seismic facies analysis

The observed thickness of the syn-rift infill varies in the study area, reaching somewhere more than 1 km (Fig. 13). Based on scattered well core data and publications conducted on outcrops, eight facies associations were defined (Table 1.) in sense of Feng (2022): Alluvial fan (A); Fan delta (B); Lacustrine (C); Volcanic rocks facies association (D); Shallow marine (E); Transitional Marine (F); Slope apron (G) and Marine offshore (H).

Alluvial fan facies association (A) was defined in wells W-4, W-5, W-6, and W-11 (Fig. 4a). It consists of two lithotypes: breccia and conglomerates, with predominantly carbonate clasts from the Neogene basement that are either clast-supported or a matrix-supported by sand, silt, or clay. Conglomerates are massively textured and poorly to moderately sorted, indicating a proximal source. They represent debris deposits (Table 1).

Fan delta facies association (B), defined in wells W-3, W-4, W-10, and
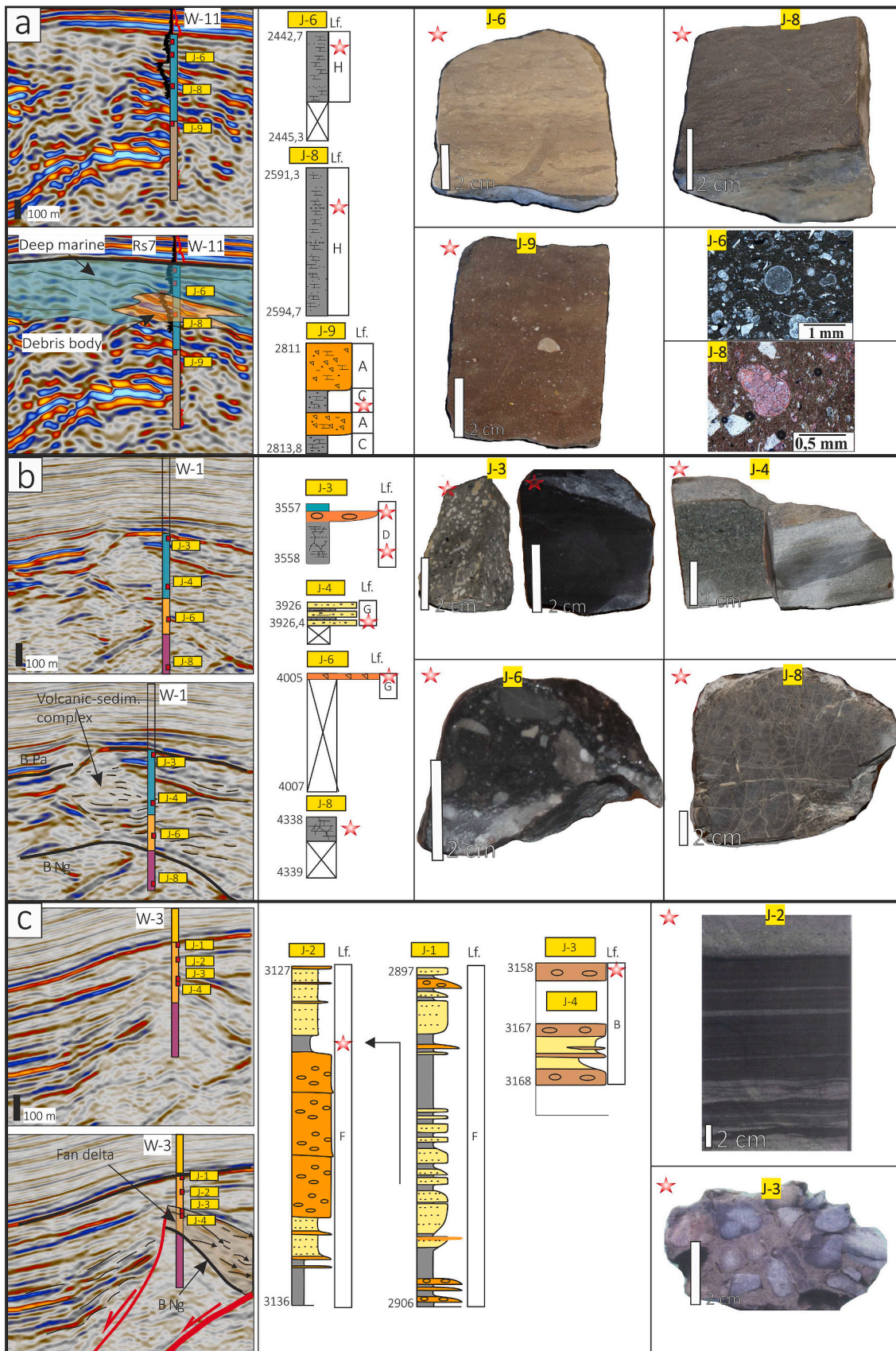
Fig. 4. Cores, thin sections, logging, and seismic reflection features of: a) prodelta or lake sediments (J-9 – Facies C), marine offshore foraminiferal limestones (J-6 *Orbulina suturalis zone* – Facies H; J-8 *Praeorbulina glomerosa zone* – Facies H); b) offshore debris conglomerates (J-6 – Facies G) and volcanic rocks interlayered with offshore sediments (J-3 – Facies D; J-4 – Facies G); c) fan delta (J-3 – Facies B) and transition to marine offshore (J-1 and J-2 – Facies F).

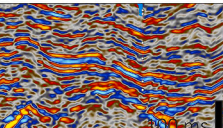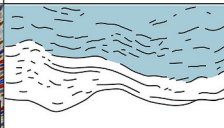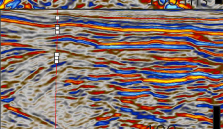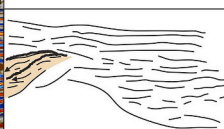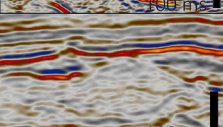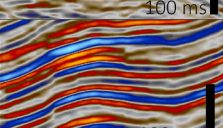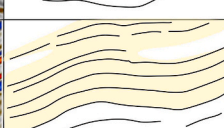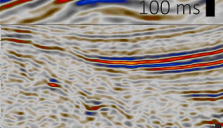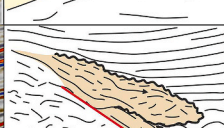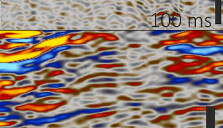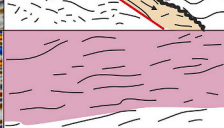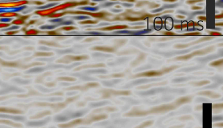| Seismic facies			Seismic examples		Lithology	
Unit	Amplitude and frequency	Spatial occurence	Seismic example	Interpretation	Facies	Depositional environments
VII- Oblique	Low to middle amplitude, low to middle frequency	Within syn-rift infill in center of the depocenters			C F G H	Prodelta or lake Marine offshore or deepwater
VI- Proximal aprons, hummocky to discontinuous	Low to high amplitude, middle frequency	Within syn-rift infill on basin slopes			B	Fan delta
V- Chaotic, hummocky to discontinuous	Low amplitude, low frequency	Within syn-rift infill as volcanic bodies			D	Volcanic rocks interbeded with syn-rift sediments
IV- Sub-parallel, continous to discontinuous	Middle to high amplitude and high frequency	Within syn-rift infill on basin edges			B E	Fan delta Shallow marine
III- Fault aprons, hummocky to discontinuous	Low to middle amplitude, low frequency	Within syn-rift infill next to boundary faults			A B G	Alluvial fan Slope apron
II- Chaotic, discontinous to partly discontinuous	Low to high amplitude, low to high frequency	Pre-rift basement above extensional detachment				Pre-rift Mesozoic to Paleozoic basement above extensional detachment
I- Chaotic discontinuous	Low amplitude, low frequency	Pre-rift basement below extensional detachment				Pre-rift metamorphic basement below extensional detachment

Fig. 5. Correlation of facies associations and seismic facies. Facies associations: Alluvial fan (A); Fan delta (B); Lacustrine (C); Volcanic rocks (D), Shallow marine (E); Transitional marine (F); Fault apron (G) and Marine offshore (H).

W-12 (Fig. 13b) consists of polymictic and monomictic conglomerates and sandstones with sporadic siltstones (Fig. 4c). Clasts are angular to subrounded and poorly sorted. They are derived from the carbonates and crystalline rocks of the Neogene basement. The matrix in conglomerates is predominantly sandy, occasionally weathered/limonitized, and clay-rich. Angular and coarse-to medium-grained matrix-supported clasts in conglomerates and sandstones suggest a proximal source (Table 1). Furthermore, occasional hematite in the matrix suggests subaerial deposition. On cutting samples, sequences S and M are mostly represented by this facies association in the form of thick conglomerate intervals (up to 150 m).

Lacustrine facies association (C) is defined in well W-11 (Fig. 4a and 13a) and consists of siltstone and silty limestone with sericite and quartz in the detritus. The fine-grained sediments of this facies can be interlayered with coarsegrained sediments of facies B of heterogeneous composition (Fig. 4a and 13a). Lithology succession on Well W-11 indicates that these facies occur in uppermost part of Early Miocene succession, on top of the facies associations A and B (Fig. 4a). Based on clast size and lithology, facies association C is defined as prodelta or lake (Table 1).

Volcanic rocks facies association (D) was defined in wells W-1, W-2, W-14, W-15, and W-16 and contains basalts and andesites (Fig. 4b and 13b, and c). This facies is observed to be interlayered with marine limestones of facies H or siltstones and sandstones of facies G (Fig. 4). In well W-1 and W-2 they reach a thickness of more than 300 m.

Shallow marine facies association (E) is defined solely in outcrop and has been described in previous studies (Pavelić et al., 1998; Sremac et al., 2016). It consists of bioclastic sediments, including biocalcarenites and biocalcirudites, with abundant corallinacea, bryozoa, molluscs, urchins, benthic foraminifera detritus, and minor planktonic foraminifera, but also silicate clasts. The clasts are cemented with calcite cement. Sandstones can be characterised by normal gradation and horizontal lamination to cross-bedding, whereas conglomerates have structures with cross-bedding. The abundant marine shallow-water fossils and sedimentary textures indicate a transitional environment between marine reef slopes and shoreface (Table 1).

Transitional marine facies association (F) (Figs. 4c and 13b, and c), determined in wells W-3 and W-13, consists mainly of marls interbedded with arenites or rudites (biocalcarenites and biocalcirudites). The sandstones are abundant with benthic foraminifera, fragments of bioclastic material, and minor siliceous material. The carbonate mudstone contains mainly benthic and subordinate planktonic foraminifera. In well W-3, it occurs on top of the facies B (Fig. 4c), or in outcrops on top of the facies E, indicating deepening. Facies F is interpreted as transitional to offshore marine environment based on the presence of benthic and planktonic foraminifera and occasional material from shallow-water environments (Table 1).

Slope apron facies association (G) (Fig. 4b and 13b, and c) is identified in wells W-1, W-8, W-10, and W-12. It contains mixed bioclastic-siliciclastic sediments of breccias, conglomerates, sandstones, siltstones,
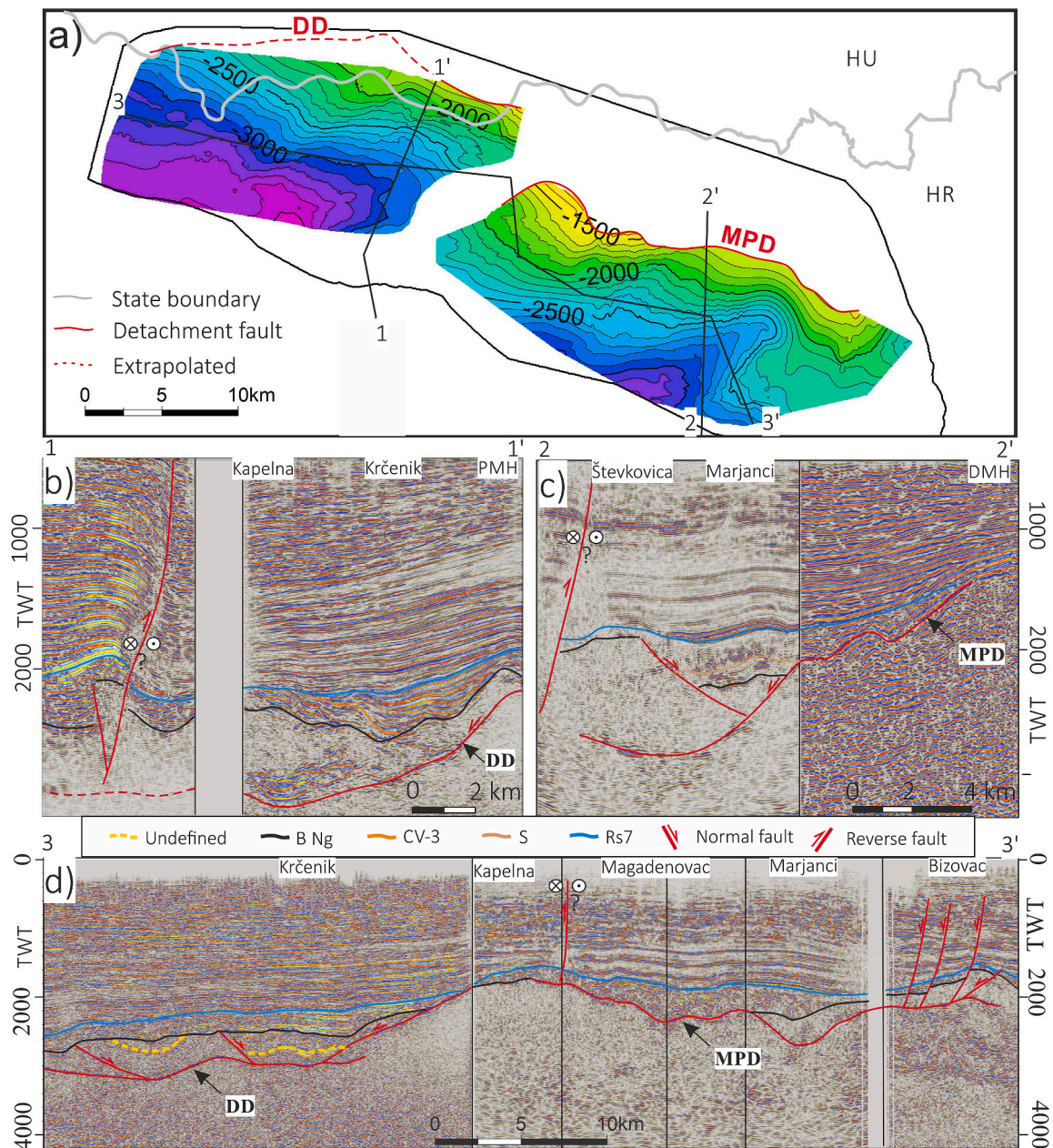
Fig. 6. Position of interpreted extensional detachments (CV and S – Tops of the Early rift sequences, Rs7 – explanation in 4.3.1. section): a) Two-way time maps of the interpreted detachments Dravica (DD) and Miholjački Poreč (MPD) b) section 1-1′ across the DD fault (*PMH* – Podravska Moslavina high); c) section 2-2′ across the MPD fault (*DMH* – Donji Miholjac high); and d) longitudinal section 3-3' across the entire study area. Location of interpreted syn-rift structures on Fig. 7.

and micritic limestone (Fig. 4b). The coarse-grained sediments contain angular or rounded metamorphic and carbonate clasts of Neogene basement, in a muddy matrix with thin fining upward intervals. The micritic limestone contains abundant planktonic foraminifera. Based on the presence of planktonic fossils in the matrix and their alteration with facies H, facies G is interpreted as a gravitational debris flow on the basin slope in marine offshore environments (Table 1).

Marine offshore facies association (H) contains homogeneous micritic limestones rich in planktonic foraminifera (Figs. 4 and 13b, and c). This facies was identified in wells W-1, W-2, W-7, W-9, W-10, W-11, W-12, and W-13. Quartz and mica clasts are sporadically present as silty detritus. These sediments were interpreted to be offshore in origin (Table 1).

The spatial distribution of depositional environments in different sequences and rift stages is examined based on the changes in seismic facies and their position in relation to the interpreted syn-rift structures.

Seven seismic facies were defined based on seismic reflection amplitude, frequency characteristics, and their spatial occurrence regarding to the syn-rift structures. Two seismic facies (I and II) were characteristic of the pre-Neogene basement, and five were defined as seismic depictions of syn-rift infill (Fig. 5).

The seismic facies III is defined as hummocky to discontinuous reflections that occur as fan aprons in the hanging wall of normal faults. Within this seismic facies, syn-rift infill is represented by facies associations A and B of alluvial fans and fan-deltas (Fig. 4c), and facies association G, which corresponds to sediments of the offshore slope apron (Fig. 4b). The seismic facies IV has subparallel, continuous, and discontinuous reflectors located within the syn-rift infill near the basin margins. For the early rift sequences, it is correlated with the transitional or fan delta facies association. In the late rift stage, it is associated with nearshore deposits in marine environments and correlated with facies E. Seismic facies V exhibits chaotic, hummocky to discontinuous
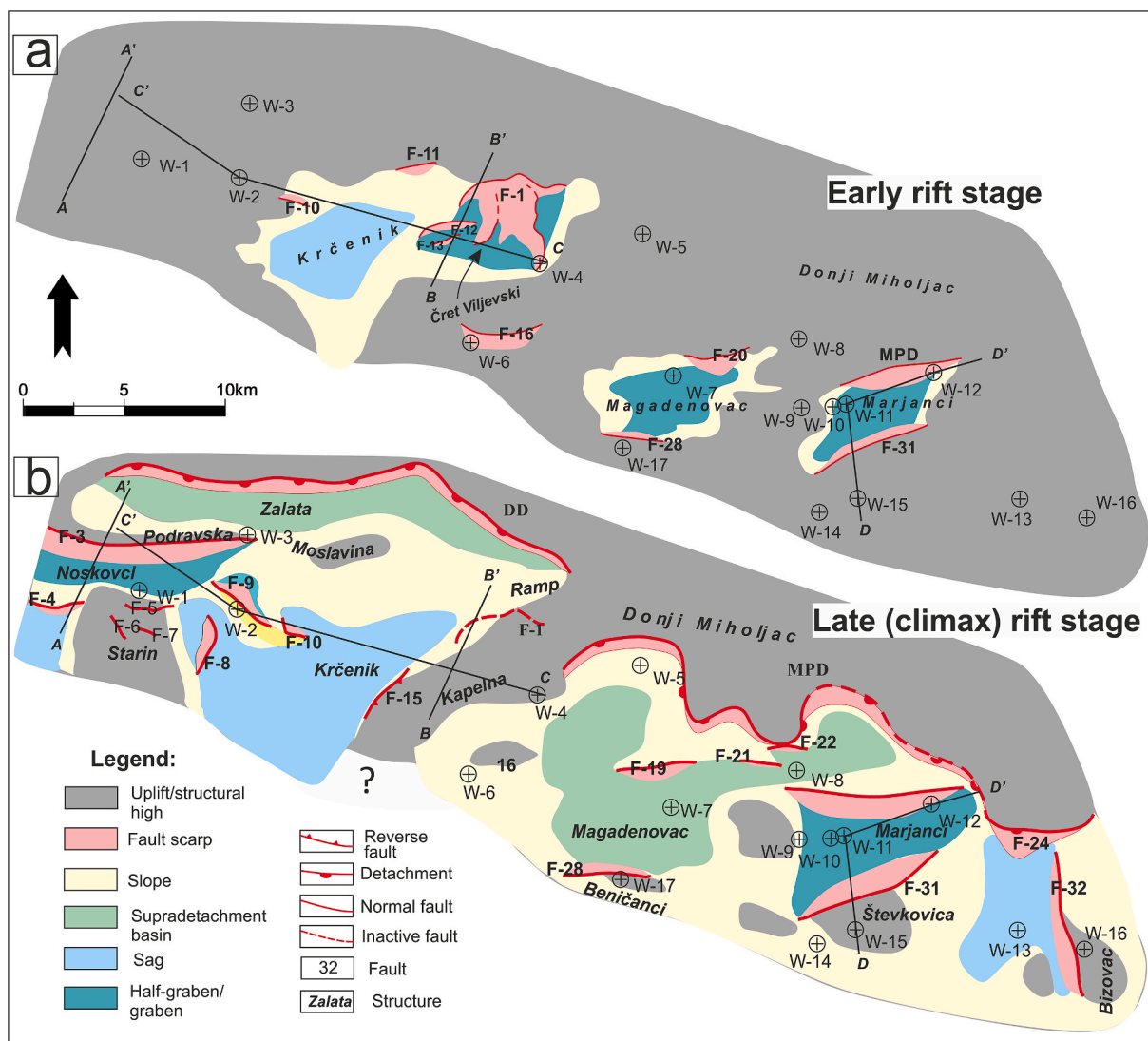
Fig. 7. Maps of interpreted tectonic units: a) early rift stage; b) rift climax stage. During the early rift stage graben structures were developed in the east, the half-graben and sag structures developed in the west, constraining small basins. Notice the shape of F-1 fault as a result of sequential tectonic activity, i.e. local rift migration. Late rift stage is characterised by formation of new structures as well as subsidence of former ones. This resulted in diverse palaeomorphology with numerous uplifts and depocentres.

reflections. Within this seismic facies, syn-rift rocks are represented by basalts and andesites of facies association D, which are occasionally interlayered by G facies (Fig. 4b). The seismic facies VI is defined as proximal aprons with hummocky and discontinuous reflections that occur on basin slopes and correlate with facies associations A and B of alluvial fan and fan-delta sediments (Fig. 4c). The seismic facies VII is characterised by oblique reflections occurring within syn-rift depo-centers where facies associations C (prodelta or lake; Fig. 4a) and F and H (transitional (Fig. 4c) and offshore marine (Fig. 4a)) occur.

4.2. Basin types and syn-rift structures

Two low-angle detachment faults and six syn-rift structures were identified: half-graben, graben, basinal sag, basinal highs, structural ramp, and supradetachment basin (Figs. 6 and 7). These syn-rift structures formed during different stages of extension. The onset of rifting was identified by the formation of spatially confined structures that included two grabens and linked sag and half-graben which constrained syn-rift deposition (Fig. 7a). Continuation of rifting was characterised by fault growth and further rift opening in such a way that existing rift structures either emerged, became embedded in the newer ones, or

continued their existence by widening and linking with the others, while most of the extension was accommodated by the Dravica detachment (DD) and the Miholjački Poreč detachment (MPD) (Fig. 7b).

4.2.1. Extensional detachments

Structural interpretation of 3D seismic revealed the presence of the NW-SE striking DD and MPD faults rising toward the Hungarian-Croatian border (Fig. 6a and see DD and MPD in Fig. 6b and c). In the northeast of the study area, DD dips SSW and reaches >3500 ms of TWT (Fig. 6a). The eastern part of the DD fault plane is curved and changes orientation so that the southeastern part dips toward the NNW and forms a synform in its hanging wall dipping westward (Fig. 6a and b). The western section of the MPD dips southward from a depth of 1500–3400 ms, dying out on the Croatian side of the Drava Basin (Fig. 6c). The easternmost section, however, forms the Bizovac antiform (Fig. 6d). Consequently, the southeastern part of the MPD is concave and forms an SW-dipping synform (Fig. 6a). The longitudinal seismic section (Fig. 6d) shows that the interpreted detachments are not structurally connected. In addition, the western section of the MPD is shallower than the eastern part of the DD (Fig. 6a and d). Both detachments are characterised by the ramp-flat-ramp geometry (Fig. 6b and c), with dips ranging from
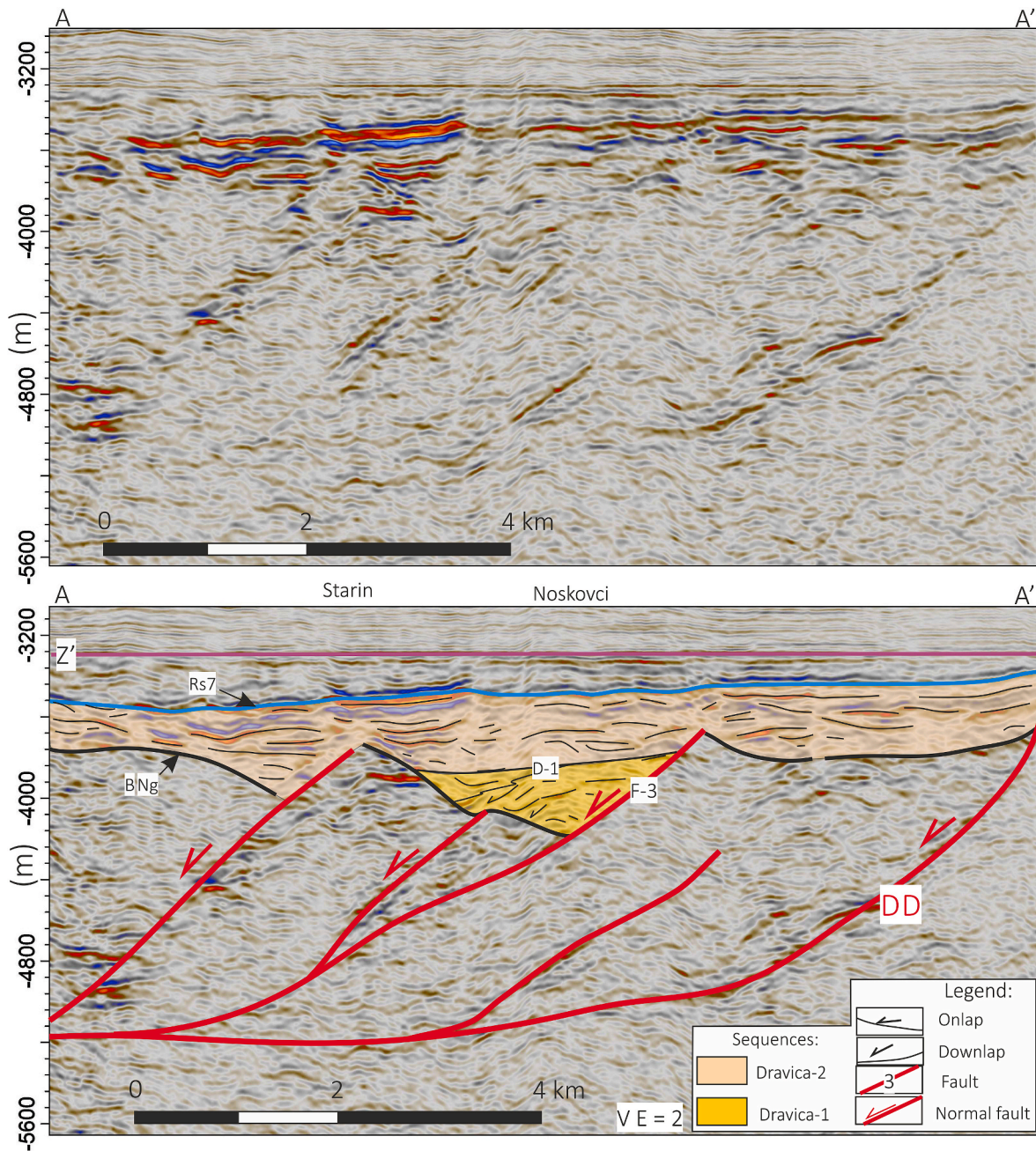
Fig. 8. Seismic cross section A-A' (location in Figs. 7 and 13), with interpreted normal faults in the hanging wall of Dravica detachment (DD). Seismic line is flattened on horizon Z.

horizontal up to approximately 25° at the ramp segment.

The seismic facies interpreted in the hanging wall is quite different from that in the footwall of the detachments (Fig. 6a, b, c, and 9). The hanging wall is characterised by chaotic discontinuous seismic facies I and fairly continuous seismic facies II, especially in the northern part of the study area, whereas the footwall contains only seismic facies I (Fig. 6b). The observed complexity of the seismic facies results from the highly variable lithology of the Neogene basement. The well data show that the detachment footwall consists of metamorphic rocks (well W-12 in Fig. 11), whereas the Neogene basement in the hanging walls is mainly composed of Mesozoic carbonate with a minor presence of younger igneous rocks. The Mesozoic carbonates are predominantly fractured carbonates (core J-8 in Fig. 4b). In addition, the morphology of the detachment surfaces indicates the uplift of antiform structures of varying sizes in their footwall. The southern flank of the Donji Miholjac

high in the MPD footwall extends into the smaller Ŝtevkovica antiform (Fig. 6a and c).

4.2.2. Half-graben structure

Initial rifting was controlled by the marginal normal fault F-1 (Fig. 7a) with three successive periods of extension, changing its orientation. The half-graben structure formed in the hanging wall is ~5 km wide. During its formation, the dip of the F-1 fault changes from west to southwest and finally to south (Fig. 7a). The half-graben tilted westward in its final phase, changing its strike from N–S to E-W. This early rift sedimentary infill is characterised by hummocky to discontinuous seismic facies III (Figs. 9 and 10).

Extension during the final stage of rifting to the west controlled the formation of the F-3 normal fault along with the narrow Noskovci half-graben in its hanging wall (Fig.. 7b and 9). This narrow E-W striking
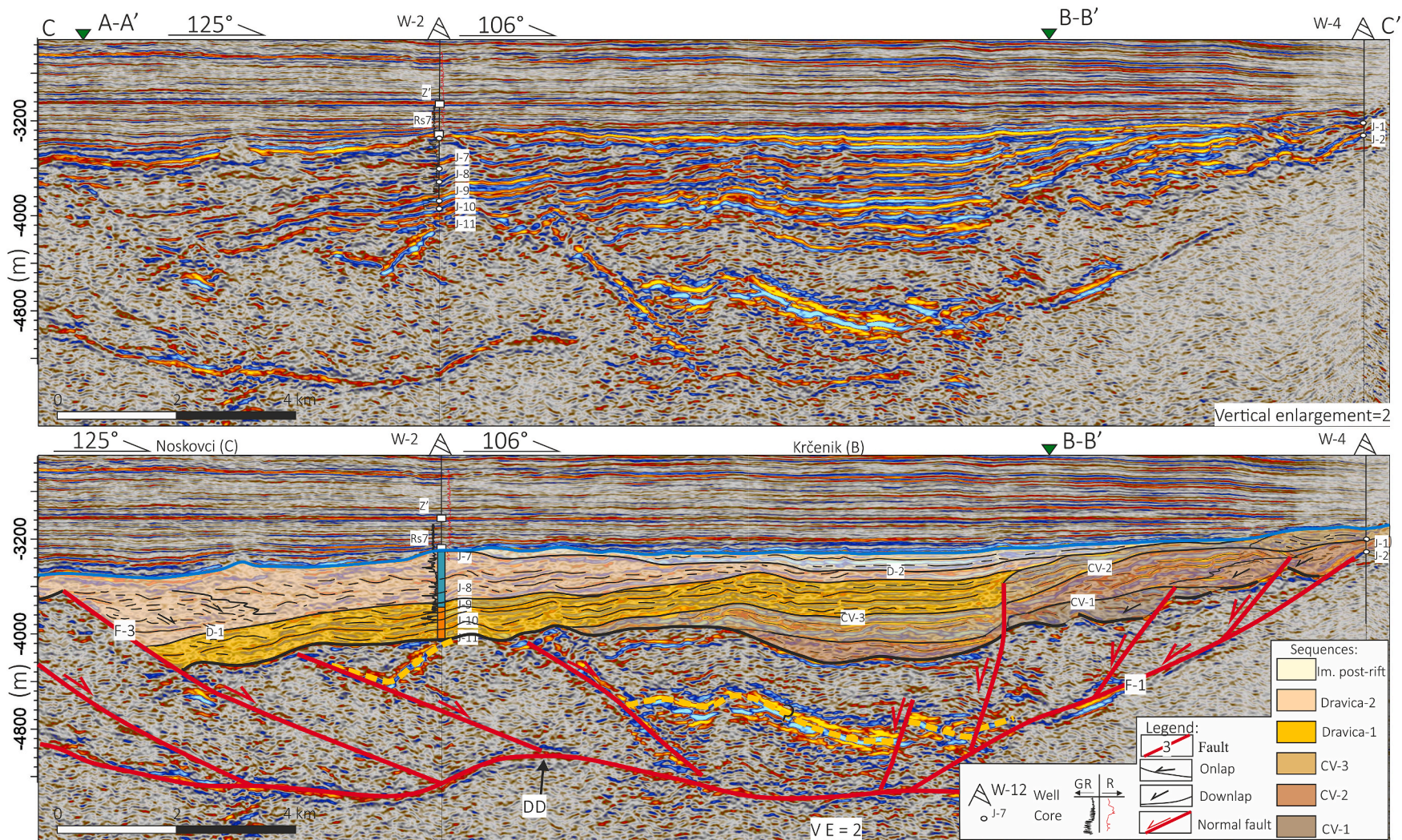
Fig. 9. Longitudinal section C–C' (location in Figs. 7 and 13; CV-1, CV-2, CV-3, D-1, and D-2 on the interpreted section refer to top of the sequence). Note the retrogradation pattern of seismic facies in the hanging wall of the F-3 fault. The seismic line is flattened on horizon Z'.

Fig. 10. Cross section B–B' (location in Figs. 7 and 13; CV-1, CV-2, CV-3, and D-2 on the interpreted section refer to the top of the sequence; IPRS – immediate post-rift). Note the retrogradation pattern of seismic facies within the third-order sequences CV in the hanging wall of faults F-1 and F-12. The seismic line is flattened on horizon Rs7.

structure is > 10 km long and only 3 km wide. The sedimentary basin fill is represented by the hummocky to discontinuous seismic facies III, chaotic, discontinuous to hummocky seismic facies V, and the oblique seismic facies VII (Figs. 9–11).

4.2.3. Graben structure

Two 5–10 km long graben structures, bounded by the E-W striking normal faults, developed during the onset of rifting south of the Donji Miholjac high (Fig. 7a and b). The Magadenovac graben lies between the F-20 and F-28 normal faults, while the Marjanci graben lies between the MPD and F-31 normal faults. The sedimentary basin fill of these depositional basins is characterised by hummocky to discontinuous seismic facies III in the direct hanging wall of the normal faults and oblique

seismic facies VI on the basin slopes in the early rift stage (Figs. 11 and 13a) and appearance of seismic facies VII in late rift stage (Figs. 11 and 13b and c). Development of the Marjanci graben development due to tectonic subsidence along the F-31 and MPD continued in the late rift stage (Fig. 7 b), linking it to the Magadenovac supradetachment over the submerged high (Fig. 7a and b).

4.2.4. Basinal sag

The Krčenik sag lies to the west of the Čret Viljevski half-graben (Fig. 7a and b). During the early rifting stage, it extended for ~10 km E-W and was ~5 km wide. Continued subsidence during the syn-rift phase extended this structure further westward by the end of the rift phase (Fig. 7a and b). It forms a synform with the DD (Figs. 6 and 7). The
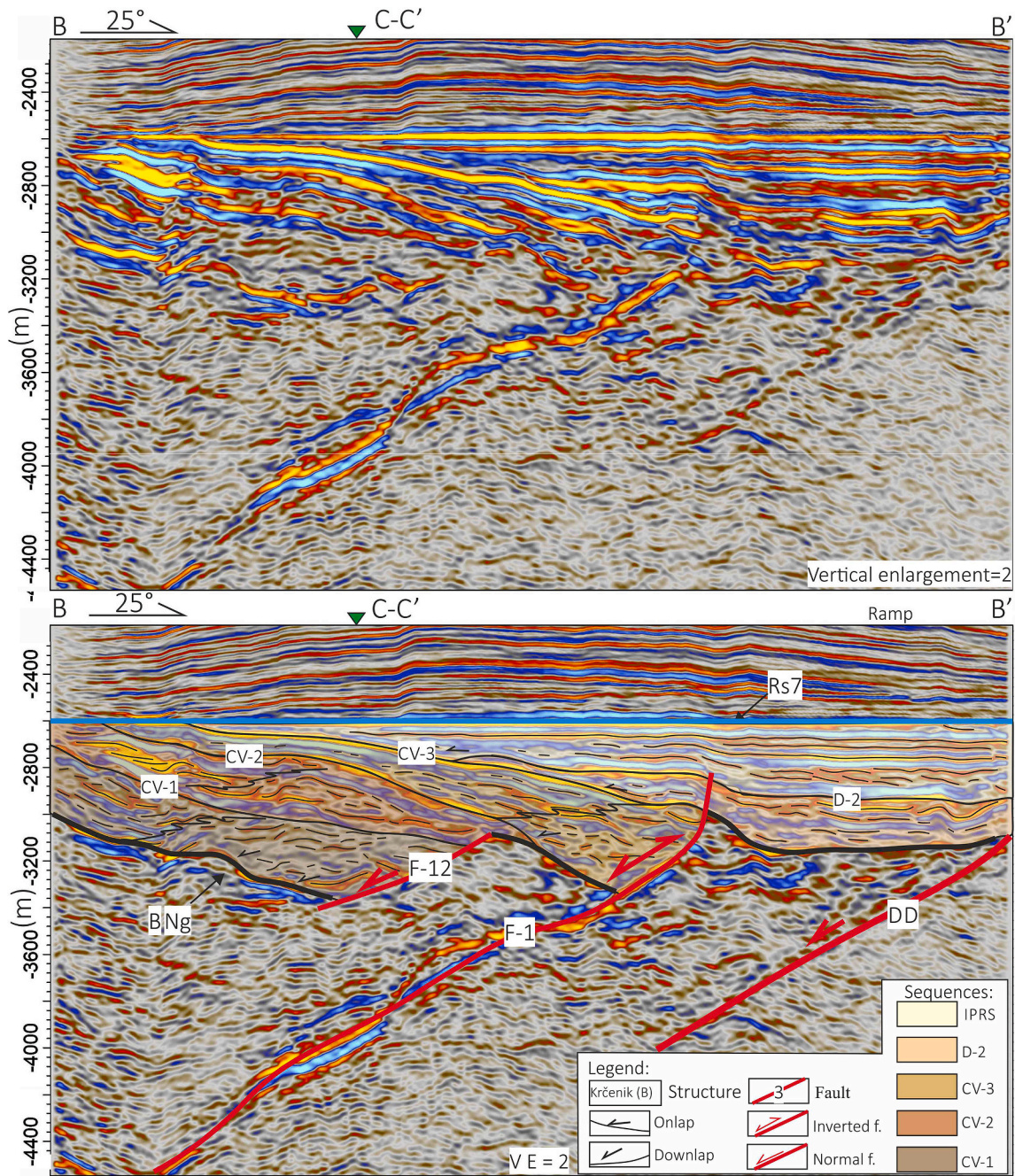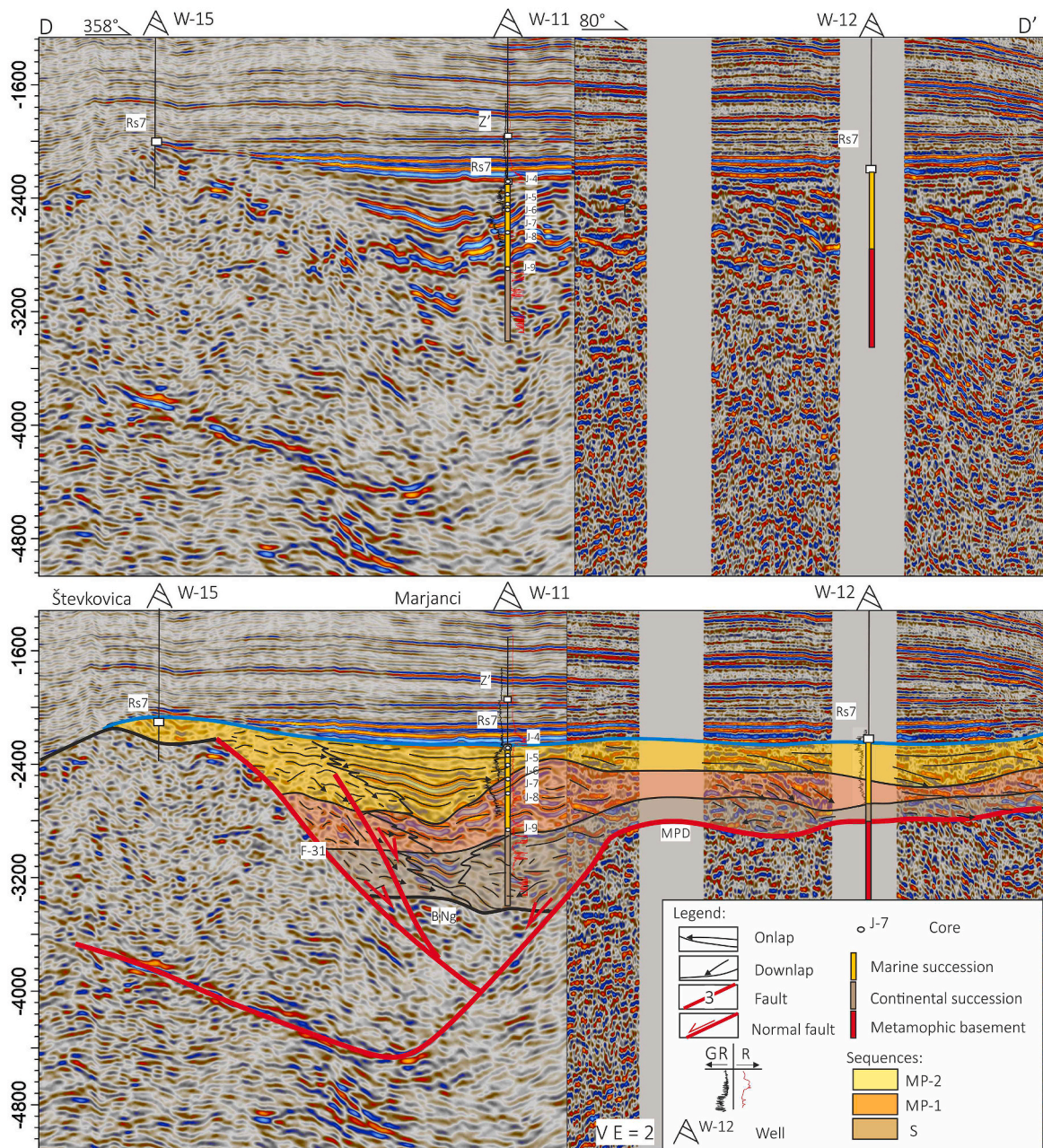
Fig. 11. Cross section D-D' (location in Figs. 7 and 13; S, MP-2, and MP-2 on the interpreted section refer to top of the sequence) in the eastern part of the study area. Note the retrogradation pattern of seismic facies within third-order sequences in the hanging wall of the F-31 fault, indicating that sedimentation is out of pace with subsidence.

400 m thick sedimentary infill is characterised by the seismic facies IV to the east and VII to the west (Fig. 9).

4.2.5. Supradetachment basin

Subsidence of the hanging wall of the late rift strata observed north of the Podravska Moslavina structural high (Fig. 6b) indicates the formation of the Zaláta supradetachment above the DD fault. This E-W striking basin is interpreted to be 20 km long and up to 5 km wide (Fig. 7), with seismic facies III observed on the southern basin slope, while the northern part is not covered with seismic.

The Magadenovac graben formed in the early rift stage became a part of the wider supradetachment basin due to the propagation of the MPD, which then became a low-angle normal fault (Fig. 6b and 7b). The connection between the Krčenik and Magadenovac depocenters in the late rift phase is not proven due to the lack of seismic data (Fig. 7b). The

transition of seismic facies IV to seismic facies VI was observed in both supradetachment structures from the margins to the central part of the depocenters (Fig. 9).

4.2.6. Relay ramp

The observed ramp formed between faults F-1 and DD as a result of their interaction. The F-1 fault formed during the early rift and is associated with the syntectonic sediments of the CV sequence (Fig. 9). The DD fault continued its activity and propagation in the late rift stage, causing tilting of the CV sequence, and interacting with the F-1 fault forming a ramp structure. Consequently, during the late rift stage, the ramp served as the main sediment transport zone from the uplifted footwall of the DD into the Krčenik sag (Fig. 7b). The sedimentary infill of this structure is characterised by the seismic facies IV and VII (Fig. 10).

Fig. 12. Multi-attribute seismic maps (overlapping RMS amplitude and variance) with interpreted sediment bodies showing distributional characteristics of the sediment transport pathways in the western part of the study area with the best 3D dataset: a) sequence CV-3 and b) sequence D-2.

4.2.7. Structural high

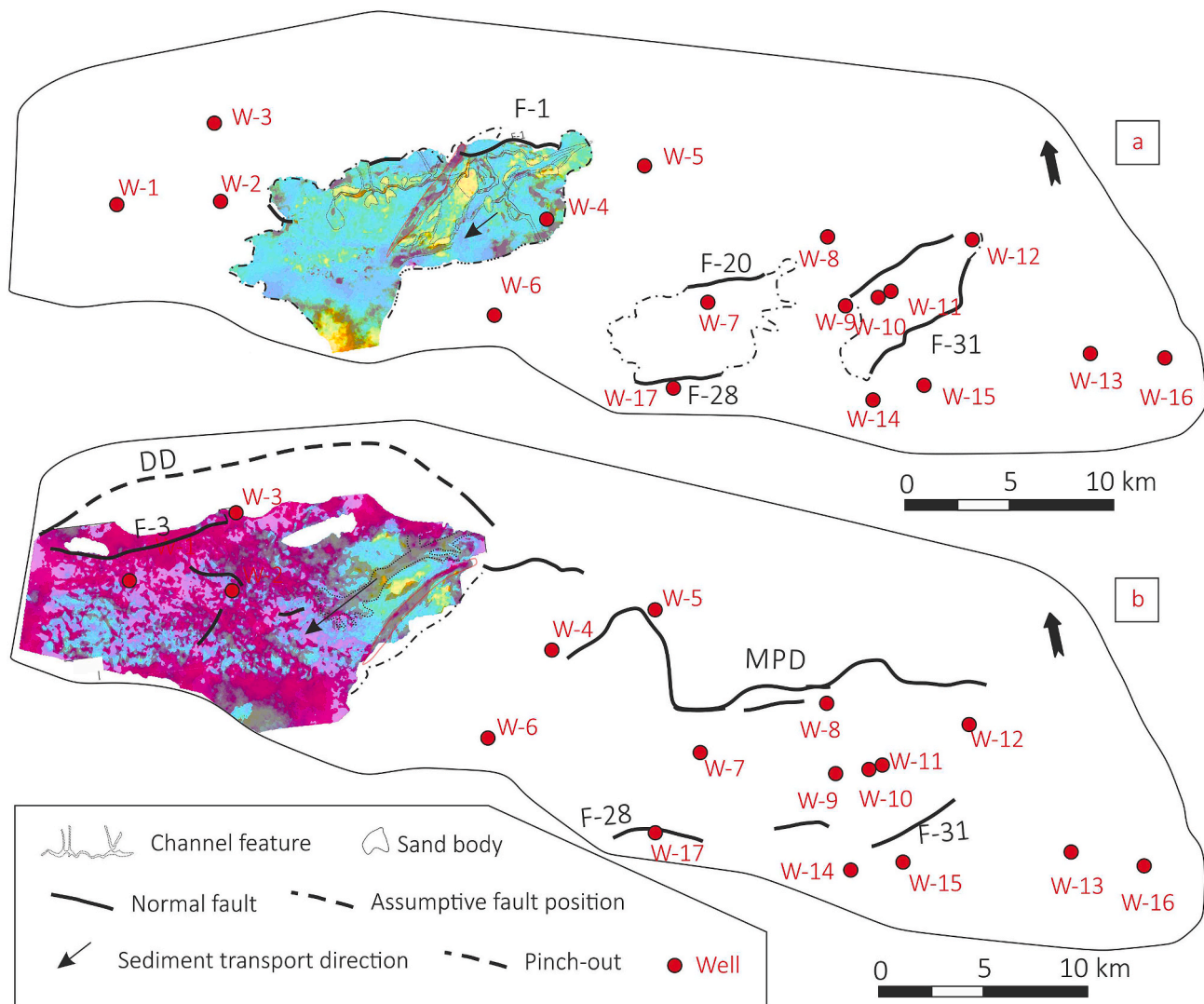The structural highs formed in both the early and late rift stages. Early rift highs formed between separate depocenters such as between the Marjanci and Magadenovac grabens (Fig. 7). In the late rift stage, highs formed in the hanging walls of newly formed normal faults such as Podravska Moslavina, Števkovica, and Bizovac or faulted palaeorelief such as the Beničanci and Starin highs. The uplift of the Kapelna high can be correlated with the boundary between the early and late rift stages (Fig. 6b) and mapped F-15 thrust fault (Fig. 7b).

4.3. Rift tectonostratigraphic sequences and depositional distribution

4.3.1. Sequence hierarchy and stratigraphic position

The syn-rift represents a single first-order sequence between the BNg and post-rift boundaries. In the Croatian section of the PBS, the BNg horizon contains two regional unconformities: the boundary between i) the Neogene succession and older, mostly Mesozoic rocks and subordinately Palaeozoic rocks, and ii) the Neogene succession and crystalline rocks. We interpret the entire BNg horizon as the base of the syn-rift. The post-rift boundary separates the syn-rift infill from the post-rift Neogene basin infill and generally coincides with the Rs7 horizon, which is the regional stratigraphic boundary between Lower or Middle Miocene and Upper Miocene rocks, as indicated by well logs (Malvić and Cvetković,

2013).

The two syn-rift stages are divided into second-order tectonostratigraphic sequences named after the major active faults that contributed to their development. In the early syn-rift, the Čret Viljevski (CV), Malinovac (M), and Števkovica (S) sequences were deposited in continental environments and controlled by faults: F-1 (Čret Viljevski fault); F-28 (Malinovac fault); and F-31 (Števkovica fault) (Fig.. 7a, 9 and 10, and 11). In the late syn-rift, the Dravica (D) and Miholjački Poreč (MP) sequences were deposited in marine environments, predominantly controlled by the activity of the DD and MPD faults (Figs. 9–11). Third-order sequences were interpreted within the CV sequence in the early rift stage, and within the D and MP sequences in the late rift stage. The sequence CV is subdivided into three third-order sequences: CV-1, CV-2, and CV-3 (Figs. 9 and 10). In the western part of the study area, sequence D was further subdivided into D-1 and D-2 (Figs. 8–10). In the east, in the hanging wall of the MPD, the sequence MP was subdivided into MP-1 and MP-2 (Fig. 7a and 11).

Biostratigraphic analysis of planktonic foraminifera from the core samples showed that sequences D-1 and MP-1 contain *Praeorbulina glomerosa* (Fig. 4a), *Trilobatus trilobus*, *Cassigerinella chipolensis*, *Globigerinoides bisphericus*, *Praeorbulina curva*, and *Trilobatus sicanus*. The presence of *Praeorbulina glomerosa* and *Trilobatus trilobus* indicates the biostratigraphic zone M5 (Hohenegger et al., 2014).
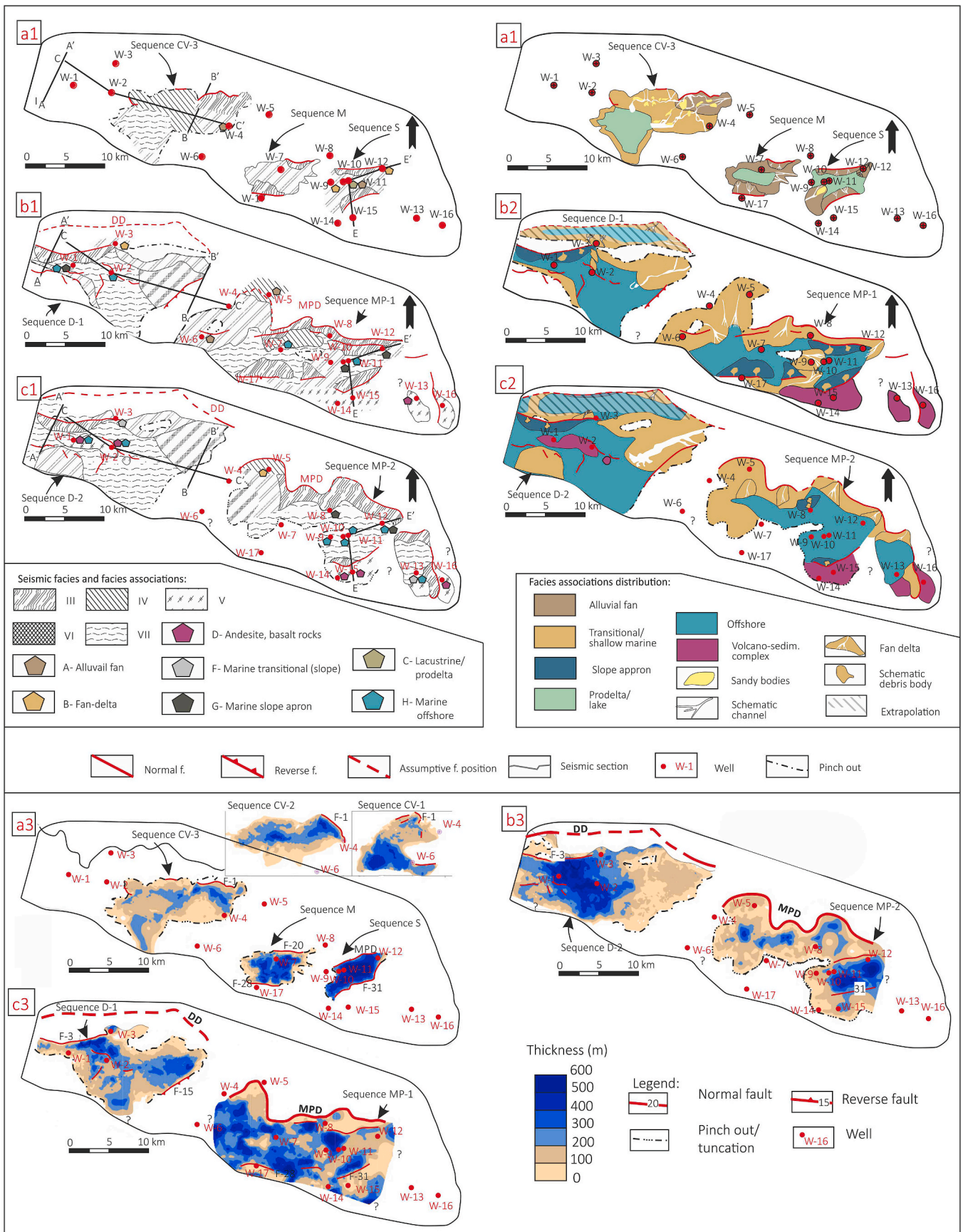
Fig. 13. The 3D seismic based tectonostratigraphic analysis of syn-rift sequences: a) CV-3, M, and S (early rift stage); b) D-1 and MP-1 (late rift stage); c) D-2 and MP-2, (late rift stage). Seismic facies distribution correlated with facies associations in wells (1); distribution of depositional systems of sequences (2); thickness maps of sequences (3); Dravica extensional detachment (DD); Miholjački Poreč extensional detachment (MPD).

Table 1
Characteristics and interpretation of facies.

Facies association	Well	Lithology	Sediment structure and texture	Fossils	Transport mechanism	Depositional environment
A	W-4	- breccia and conglomerate	-massive	–	- rockfall/debris flow	-alluvial fan
B	W-3, W-11	- polymictic breccia-conglomerate - sandstone - siltstone and mudstone	- massive, graded bedding	–	- debris flow	-fan-delta
C	W-11	- silty limestone - siltstone	–	–	?	-prodelta/lake
D	W-1, W-2	- andesite - basalt	–	–	–	
E	Defined in outcrops	-reef limestones - biocalcarenites and biocalcirudites	-normal graded bedding - horizontal lamination, - cross-bedding	-benthic foram., - fragments of Corallinaceae, bryozoans and pelecypods, - less planktonic foram.	- flow regime, - subaquatus dunes	-shoreface
F	W-3, W-13, W-14	- sandstone, - conglomerate - biocalcirudites, - biocalcarenites - marl	-horizontal lamination, - gradation, - massive	-benthic foram - planktonic foram., - fragments of Corallinaceae, bryozoans and pelecypods	-suspension, - turbidity currents	- lower shoreface - offshore
G	W-1, W-8, W-12	-breccia, - conglomerate, - sandstone, - siltstone, -limestone	- massive, - gradation	-planktonic foram. - subordinately benthic foram.	-turbidity currents	-slope (fault) apron
H	W-1, W-2, W-9, W-10, W-11, W-12	-micritic and silty limestone	-massive	-planktonic foram.	-suspension	- offshore

Sequences D-2 and MP-2 contain abundant *Orbulina suturalis* (Fig. 4a), *Orbulina universa*, *Trilobatus trilobus*, *Globigerina diplostoma*, *Tenuitella angustiumbilicata*, *Globorotalia mayeri*, *Globorotalia scitula*, and *Globigerina bulloides*, indicating the continuation of marine offshore environments in the central part of the depocentre. However, the abundance of *Orbulina suturalis* and *Orbulina universa*, and absence of the *Trilobatus bisphericus* indicate the younger biostratigraphic zone M6 (Hohenegger et al., 2014).

4.3.2. Seismic sedimentary characteristics of the early rift stage (sequences CV, M, and S)

Three spatially separated basins developed during the early rift stage in continental sedimentary environments. The second-order CV sequence was deposited in the Čret Viljevski half-graben and in the Krčenik sag (Fig. 7a). The second-order M and S sequences were deposited in the eastern area in the Magadenovac and Marjanci grabens (Fig. 7a). The activity of the F-1 fault subdivided the CV sequence into three third-order sequences, each of which is genetically related to one of the phases of F-1 activity. The superposition of the third-order sequence CV-1 indicates that it was formed at the beginning of the rift stage. This sequence is presented with the hummocky to discontinuous seismic facies III downlapping on the BNg surface and interpreted as alluvial fan deposits (Fig. 10). Progressive rifting during the development of the CV-2 sequence is characterised by fault back-stepping (Fig. 10), caused by the propagation of the F-1 fault, which became a major active fault in the western part of the study area. Seismic facies III was observed in the fault area, facies IV on the slope between the fault scarp and the Krčenik sag (Figs. 9 and 10), while seismic facies IV was observed westward, and interpreted solely in the Krčenik sag (Figs. 9 and 10). The change of seismic facies III to VI indicates the more developed alluvial system from gravity flows to fluid flow sediments.

The seismic appearance of the CV-3 sequence is similar to that of the CV-2 sequence. This unit is formed by continuous extension along the F-1 fault and is therefore characterised by hummocky to discontinuous seismic facies III in the immediate hanging wall attributed to gravity flow sediments (Figs. 10 and 13a). The seismic facies VI was observed on the basin slopes, while the subparallel to parallel seismic facies IV and

subordinate VII are found in the central part of the Krčenik sag. This indicates further development of the alluvial system toward the sag structure, where the alluvial gravity flow transitions to the fluvial flow and eventually to the prodelta or more likely a lake environment (Fig. 13a). Seismic attributes show channel shapes branching toward the Krčenik sag as visible 'sandy' bodies on the attribute map (Fig. 12a). In addition, after the extension along the F-1, a northward migration of the depocenter is observed (Figs. 10 and 13a).

In contrast to the CV sequence, the M sequence showed no higher-order internal subdivisions. It lies between normal faults F-20 and F-28 (Fig. 7a) and shows downlapping seismic facies III in the hanging wall (Fig. 13a). Away from the interpreted normal faults, the basin slopes are characterised by oblique hummocky seismic facies VI (Fig. 13a). The seismic appearance of sequence S is similar to that of sequence M. A hummocky to discontinuous seismic facies III was observed in the hanging walls of normal faults F-31 and MPD (Figs. 11 and 1aa). Oblique to hummocky seismic facies VI was observed on basin slopes away from these normal faults (Fig. 1a). The appearance of the seismic facies III is interpreted here as deposits of rock fall and alluvial fan (gravity flows), whereas VI is interpreted as an alluvial fan (fluid flows) sediment that transition to prodelta or lake deposits in the uppermost part of these sequences (Fig. 13a).

4.3.3. Seismic sedimentary characteristics of the late rift stage (sequences D and MP)

During the late rift stage two second-order sequences were deposited in marine sedimentary environments. Each of these sequences is subdivided into two third-order sequences. Sequence D-1 can be mapped in the western part of the study area and pinches out toward the east. Seismic facies III was observed in the hanging wall of the F-3 fault as slope apron facies, while seismic facies VII was observed westward within the half-graben and sag infill indicating offshore conditions (Figs. 9 and 13b). The southern margins of the Noskovci half-graben and the Krčenik sag are covered with seismic facies VI (Fig. 13b), while the eastern part of the Krčenik sag is filled with seismic facies IV (Figs. 9 and 13b), which are correlated with transitional environments, i.e., fan delta deposits. Above this interval, seismic facies VII and V may occur (Fig. 4b,

9 and 13b), indicating further offshore transgression and volcanic rocks presence. The visible Neogene succession in the Zálata basin (Fig. 4c) starts with the steeply dipping reflectors of seismic facies VI from the northern slope of the Podravska Moslavina high indicating fan delta deposition (Fig. 4c and 13b). This sequence is characterised by a marine offshore environment in the western part of the Krčenik sag and in the Noskovci half-graben (Fig. 13b). The main sediment source was located east of the Podravska Moslavina high, with a sediment entry point along the relay ramp northeast of the Krčenik sag, which is presented with seismic facies IV (Fig. 7b and 13b). To the east, the MP-1 sequence is characterised by a complex distribution of seismic facies due to several active faults. The western part of the sequence is represented mainly by the seismic facies VI, with a local occurrence of the seismic facies IV around well W-5 (Figs. 11 and 13b). This is related to sediment supply by fan deltas at the basin margins. The central part is dominated by seismic facies VII which indicates offshore conditions, while seismic facies III occurs in the hanging walls of active normal faults in the form of slope aprons (Fig. 13b). In addition, the Števkovica structural high and the easternmost area at the Bizovac structure are characterised by the occurrence of seismic facies V (Fig. 13b). Offshore conditions are interpreted in the Marjanci graben and the Magadenovac supradetachment basin (Fig. 7b). Because both depocenters are only 5–10 km wide, mass-waste sedimentation (of slope aprons) in the hanging walls of the normal faults (Fig. 13b) has a strong influence on the seismic signal presented with seismic facies III. Seismic facies and well data indicate that eroded material from the Donji Miholjac high was deposited in the Magadenovac depocenter through the fan delta systems in the western part of the sequence (Fig. 13b).

The seismic facies distribution of the D-2 sequence is similar to that of the D-1 sequence. In the hanging wall of the F-3 normal fault, the seismic facies III was observed as slope apron sediments (Figs. 9 and 13c). Seismic facies VII and V are distributed in the Noskovci half-graben and in the western part of the Krčenik sag indicating offshore conditions and volcanic activity (Fig. 13c). The eastern part of the Krčenik sag is covered with seismic facies IV as well as relay ramp where delta-like features are observed on the seismic attribute map (Fig. 12b and 13b). The slopes of the structural highs away from the fault slopes are covered by the seismic facies VI. Most of the sequence around wells W-1 and W-2 is marked with seismic facies V (Figs. 9 and 13c). The succession above seismic facies VI in Zálata supradetachment basin is interpreted as seismic facies VII, which is defined as the transition of a fan delta into marine offshore sediments (Fig. 13c). Sequence D-2 is characterised by marine offshore sedimentation which prevailed in the half-graben and western part of the sag (Fig. 13c), while the ramp structure still served as the main sediment entry (Fig. 13c). In the same phase, the Zálata supradetachment basin is characterised by overall transgression. Another third-order sequence MP-2 developed in the hanging wall of the MPD (Fig. 11), which is characterised by further marine transgression on structural highs due to MPD propagation (Fig. 13c). The Marjanci graben is characterised by the spatial occurrence of the seismic facies VII, which indicates offshore conditions (Fig. 13c). The seismic facies III is interpreted as slope apron fill in the hanging wall of the MPD (Fig. 13c). The structural high to the southeast continued to show volcanic activity (Fig. 13c). Three-dimensional seismic data are not available for the NE portion of the sequence therefore, interpretation is based on the available 2D seismic data. The MPD shows slight variations in dip direction and dip angle along strike, which affects changes in the depositional environment (Fig. 13c).

5. Discussion

The study of the syn-rift rock infill in the eastern part of the Drava Basin has revealed the formation of six types of syn-rift structures and two extensional detachments characteristic of continental rifting (Friedmann and Burbank, 1995; Peacock et al., 2000). Half-graben, graben, and sag structures in the early rift and their further

development in the late rift stage with the development of new structures such as ramps and supradetachment structures, separated by structural highs. This led to the evolution of continental alluvial and lacustrine environments in the early rift into the marine environments with coeval and spatially differentiated depositional systems (Figs. 7 and 13). The basin infill consists of several tectonostratigraphic units of a different order (Figs. 9–11). Seismic features correlated with well data define the style of extension and spatial distribution of depositional environments that contributed to the tectonostratigraphic reconstruction. This reconstruction can be used to predict the distribution of prospective sites for hydrocarbon exploration, deep aquifers, and geological storage of CO_2. Understanding the nature of sand body occurrence is crucial for reservoir exploration (Richards and Bowman, 1998; Tan et al., 2017). Coarse-grained sediments of the syn-rift infill have always been reservoir rocks of interest in the SW part of the PBS, as hydrocarbon accumulations are also found in them (Lučić et al., 2001; Saftić et al., 2003), with marls and clay-marls of the post-rift deep Lake Pannon (Sebe et al., 2020) directly above them as regional seals (Dolton, 2006). For these reservoirs, the novel palaeogeographic and paleostructural reconstructions and understanding of depositional constraints on reservoir conditions in the Croatian part of the PBS were lacking (Lučić et al., 2001; Pavelić, 2001; Saftić et al., 2003; Zečević et al., 2010). Moreover, this is the first case of tectonic control of syn-rift infill observed from subsurface data in the SW part of the PBS.

5.1. Sequence architecture evolution

Complex tectonic activity manifested in episodic tectonic movements, lateral tilting, and migration of depocenters, characteristic of continental rift basins (Wu et al., 2019), is evident in the studied syn-rift infill. These packages are genetically linked to tectonic control of the depositional system. Based on the differences in depositional environment, processes of fault growth, and rift opening, we observe the two stages of rift evolution in the Drava Basin. During the early rift stage, continental synsedimentary deposition was controlled by a spatially confined fault system (Fig. 13a). Sedimentation started in small graben and half-graben structures, but also sag structure is observed. Extension during the late rift stage resulted in marine deposition controlled by subsidence along low-angle normal faults (i.e. extensional detachments; Fig. 13b and c), as indicated by the formation of supradetachment basins. Therefore, the tectonically driven sedimentary record of the syn-rift depocenters cannot be correlated with Miocene transgressive events; this is also supported by stratigraphic and thermomechanical/numerical modelling in the PBS (Balázs et al., 2021). The characteristic feature of the entire syn-rift phase was the formation of relatively small but diverse types of extensional structures, from half-grabens to supradetachment basins (Fig. 15).

5.1.1. Early rift stage

During the early syn-rift stage, the CV, M, and S sequences developed in small separate depositional basins filled with alluvial fans, fan deltas, and presumably lacustrine deposits. Alluvial fans were deposited along the fault scarp slope, while fan-deltas were deposited on the fault scarp and basin slope (Fig. 13a and 15). Prodelta or lake sediments were deposited either in the central part of the interpreted grabens or in the sag depocenter (Figs. 7 and 13a).

The succession of the Lower Miocene consists of second-order sequences CV, M, and S. The second-order sequence CV was deposited in the hanging wall of the F-1 fault and within the sag structure (compare Fig. 7a with 13a). Other second-order sequences were deposited in the eastern part of the study area: the M sequence in the hanging wall of the F-28 and F-29 faults and the S sequence in the hanging wall of the F-31 and MPD faults (Fig. 7a and 13a). In contrast to the M and S sequences, the CV sequence contains multiple third-order sequence boundaries (Figs. 9 and 10). The unconformable portion of these boundaries can be identified by the erosion of the footwall, which was observed as coeval

deposition in the adjacent hanging wall of the major F-1 normal fault (Fig. 10). The interpreted sequences defined by these stratigraphic boundaries are relatively thin and show constant migration of depocenters (Fig, 13a).

All sequences show a retrograding pattern (Figs. 10 and 11), likely due to a higher rate of ongoing tectonic subsidence compared to the rate of sediment supply during most of the early rift. This may be due to cyclic subsidence caused by fault prolongation and dip change, which resulted in migration of depocenters (Figs. 7, 10 and 11). The upper boundary of the early rift stage in the western part (CV-3; Fig. 9) is unconformable and shows deformation and erosion of these sequences due to tilting of the low-angle DD fault hanging wall. This could lead to a hiatus between the continental and marine (or Early and Middle Miocene) sediments, as observed at several outcrops of the SW part of the PBS (Csontos et al., 2002; Mandić et al., 2012).

5.1.2. Late (climax) rift stage

Tectonostratigraphic observations indicate that the Middle Miocene syn-rift succession is bounded by a second-order sequence boundary. The D sequence developed in the western part of the study area is controlled by the activity of DD, whereas the MP sequence in the east is controlled by the MPD activity (Fig. 13b, and c). Both sequences contain third-order sequence boundaries indicative of higher-order tectonic cycles. The D-1 sequence exhibits a retrogradational pattern indicating strong tectonic subsidence that exceeded sediment supply (Fig. 9). It is characterised by the formation of depocenters in the western part within the half-graben and sag structures separated from the supradetachment basin by the structural high (Fig. 7b and 13b). Sequences D-1 and MP-1 were separated by the Kapelna high (Fig. 7b and 13b). The uplift of the Kapelna high (Fig. 6b) can be explained by local uplift of the tectonic block between DD and MPD (Fig. 7). Another explanation is the possible short inversion associated with a hiatus at the transition from continental/fluviolacustrine to marine sedimentation observed elsewhere in the SW part of the PBS (Mandić et al., 2012). The sequence MP-1 shows a retrogradational pattern (Fig. 11), indicating a strong tectonic subsidence that exceeded the sediment supply in the depocenters in the eastern part. Planktonic foraminifera was abundant suggesting the Badenian stratigraphic zone M5 (Cicha et al., 1998; Hohenegger et al.,

2014) (Fig. 14).

The D-2 and D-1 sequences were separated in the western part of the study area by a third-order boundary (Fig. 9), showing transgression on the basin slopes of structural highs (Fig. 13c), as indicated by the retrogradational stacking patterns (Fig. 9). The D-2 sequence was further separated from the depositional area of the MP-2 sequence by the Kapelna high (Fig. 13c), although connections between them probably existed to the south. Within the MP-2 sequence, a retrogradational stacking pattern was observed in the graben structure in the eastern part (Fig. 11). This sequence is characterised by mild northward migration of the depocenter, following MPD propagation (Fig. 13 b and c). The presence of planktonic foraminifera indicates the younger biostratigraphic zone M6 (Hohenegger et al., 2014) (Fig. 14).

5.2. Style of extension and tectonic controls on syn-rift sequences in the study area

The syn-rift tectonostratigraphic sequences are the result of the migration of fault activity, but were also influenced by rift setting (Figs. 6 and 8). Migration of depocenters can be correlated with the observed relationship between rift architecture and lithospheric strength (Pérez-Gussinyé et al., 2020). The presence of extensional detachments and metamorphic rocks forming highs in their basement supports core-complex-type extensions in the study area during syn-rift phase. Such a style of extension has been observed thought PBS (Tari et al., 1992; Horváth, 2012; Balázs et al., 2016) and in other continental rift settings (e.g. Lister and Davis, 1989; Ritts et al., 2010), but is contrary to the previously interpreted extension driven by dextral transcurrent displacement along NW-striking faults in the southern PBS (Jamičić, 1995; Lučić et al., 2001). The general southward movement of tectonic blocks (Figs. 7, 8, 10, and 11) is consistent with observations in the Hungarian part of the PBS (Balázs et al., 2016). We conclude that extension in the studied part of the Drava Basin was accommodated by extensional detachments that developed along inherited weak zones characteristic of the back-arc setting of the PBS (Fodor et al., 2021). These zones were previously formed during Cretaceous-Paleogene collision between the Adria Microplate and the European foreland along regional reverse faults or nappe systems (Balázs et al., 2016),
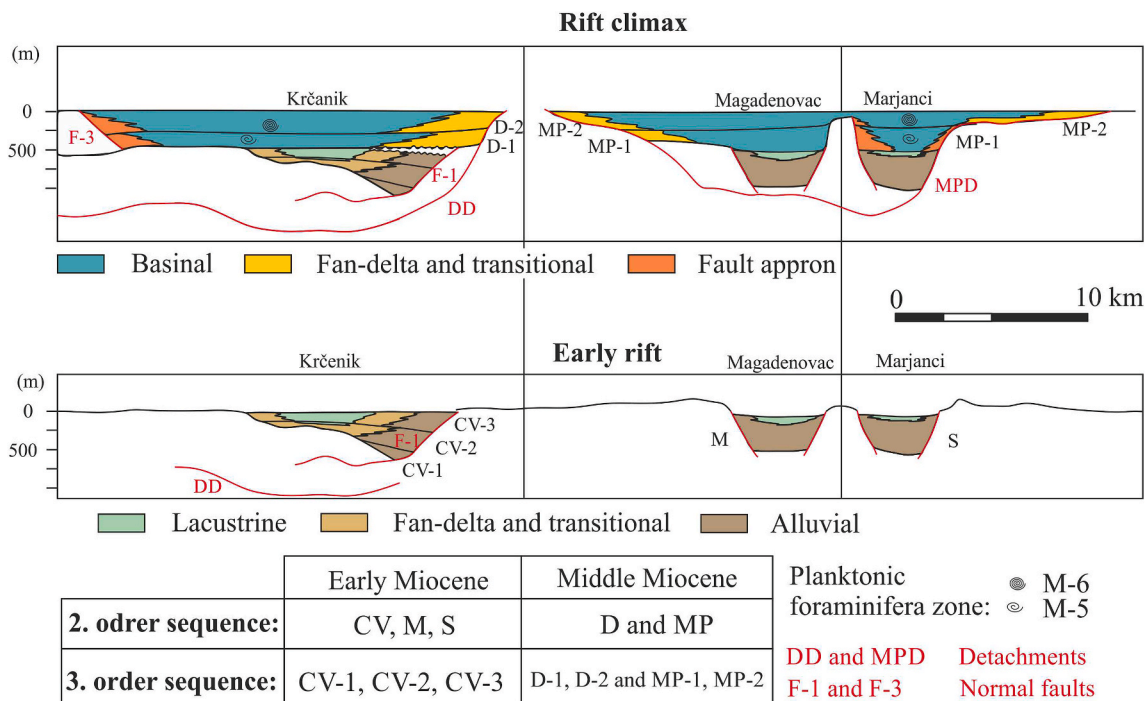

Fig. 14. Syn-rift architecture on a generalized section of the eastern part of the Drava Basin. For the location and type of structures see Fig. 7.
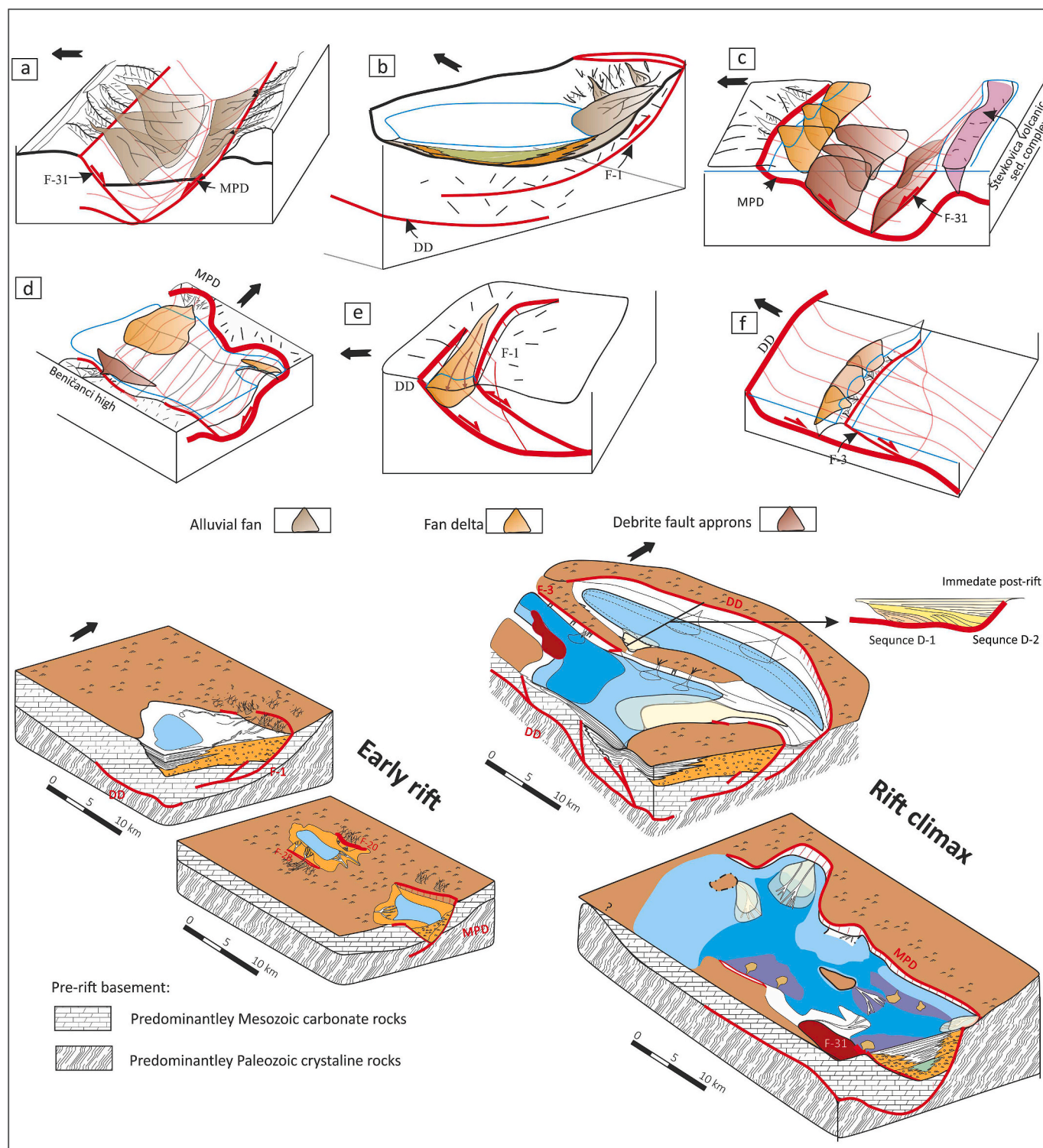
Fig. 15. Sediment transport zones and their control on the distribution of depositional environments in the study area in continental environments (not to scale): a) fault scarps in confined depositional system, b) wider depositional system of linked sag and half-graben structures, c) fault scarps in graben structure, d) fault scarps in supradetachment structure e) structural ramp, and f) a retreating detachment hanging wall.

similar to the Sava suture area on the Motajica Mt. (Ustaszewski et al., 2010). Both interpreted detachment surfaces (DD and MPD) are dipping to SSW. Their continuation in the western part of the Drava Basin (Fig. 2) could be either by S or SW dipping normal faults forming a fault zone with continuous orientation, or by NE dipping normal faults indicating a rift system composed of accommodation zones (Rosendahl, 1987). In this sense, further study of the Drava Basin is needed to obtain a

complete model of the crustal extension during the opening of the PBS. We define the observed detachment faults as part of the Drava Rift Fault System (DRFS) to distinguish it from the Drava Fault Zone (DF), which has been characterised by reverse and dextral faulting since the Pliocene. The extensional detachments are characterised by ramp-flat-ramp geometry that contributed to the overall distribution of the syn-rift infill. Inherited drainage systems may influence the syn-rift facies distribution

(Ford et al., 2017; Leppard and Gawthorpe, 2006). The sediment transport directions observed from the attribute maps (Fig. 12) are oblique to the orientations of the interpreted extensional detachments, but parallel to the Late Cretaceous trust sheets (Fig. 2). This leads to the observation that the main sediment pathways in Drava Basin may resemble antecedent drainage affecting facies distribution through the syn-rift.

5.2.1. Tectonic control in continental environments

Three mappable isolated fluvial-lacustrine basins, characteristic of the early syn-rift stage, (Fig. 7a and 13a) (Gawthorpe and Leeder, 2000; Santos et al., 2014; Ford et al., 2017; Jia et al., 2019) are delineated. This is in accordance with defined continental environment (freshwater and lacustrine depositional environments) prevailed during the Early Miocene (Pavelić and Kovačić, 2018). Infill of these basins is largely presented by the downlapping chaotic seismic facies III on fault-related slopes correlated with alluvial fan facies association, suggesting these sediments prevailed during the early rift. Alluvial fans were directed towards the centre of the depocenters on opposing fault slopes of interpreted graben structures in the eastern part (13a, 15a). In the western part, the same facies developed in the half-graben, but are also characterised by the change to the continuous, high amplitude subparallel seismic facies IV. This indicates the transition from the alluvial fan to the fan-delta and prodelta facies towards (Figs. 12 and 13a) the sag basin. A similar seismic feature has been demonstrated in other tectonic active basins (Zhu et al., 2014), reflecting the distribution of conglomerate lithofacies, with more distal areas of strong and continuous seismic reflection having better reservoir characteristics. (Tan et al., 2017).

5.2.1.1. Confined continental depositional system controlled by single rift structure.
Sequences M and S are characterised by confined and isolated alluvial-lacustrine basins that developed in small graben structures in the eastern part (Figs. 11, 13a and 15a). Alluvial fans were initially deposited in the prodeltaic plain and later within the enclosed lake directly from steep fault slopes (Fig. 13a). Sandy limestone without marine fossils was deposited in the uppermost part of this succession, suggesting lacustrine sedimentation (Fig. 4a). These confined sedimentary basins developed within one syn-rift structure and were most likely surrounded by the high-relief Mesozoic carbonate massifs (Tišljar, 1993), which yielded a variety of coarse clastic sediments.

5.2.1.2. Wider continental depositional system controlled by the multiple rift structures.
In contrast to the depocenters developed in the graben structures in the eastern part, in the western part of the study area a depositional system is characterised by episodic tectonic activity and successive subsidence that developed in the connected half-graben and sag structures (Fig. 13a and 15b). Here, the alluvial fan and fan delta sedimentation was observed in the direction of the sag structure (Fig. 13a and 15b). The sand bodies between the channel features (Fig. 12a) may show vertical and lateral changes in fan delta lithology. These sediments correlate with (sub) parallel to discontinuous seismic facies IV in the lower part and the seismic facies VI in the upper part (Fig. 9). A low-angle seismic reflection indicates a shallow-water delta of the Hjulström type (Postma, 1988). Subsidence and development of the sag suggest that DD fault playes role (Fig. 15b). This resulted in episodic development and spreading of the depositional systems. In contrast to the confined depositional system, controlled by a single observed structure, the wider deposition developed through the linking of more than one syn-rift structure – Krčenik sag and Čret Viljevski half-graben. We argue that simply by linking more rift structures enough depositional space was developed to accommodate a wider water body (lake) and a fan-delta system.

5.2.1.3. Alluvial fans on fault scarp.
Alluvial sediments deposited in continental environments are characterised by predominantly coarse-grained sediments with rapid vertical and lateral changes (Pavelić and Kovačić, 2018). These changes can be shown on seismic attribute maps (Fig. 12a) as channels branching off the F-1 fault (Fig. 13a). Well data from the grabens in the eastern part (Fig. 4a) indicate alluvial fan sedimentation in the Lower Miocene. The fault slopes in these structures were steeper than those of the coeval half-graben structure in the western part, where the main normal fault is interpreted as a reactivated pre-rift discontinuity (Figs. 9 and 15b). These alluvial fan deposits are represented in the seismic data by wedge-shaped progradation reflections of hummocky to discontinuous seismic facies (Fig. 10). Braided alluvial fans caused by successive normal faulting (Pavelić and Kovačić, 1999) can be correlated with interpreted alluvial deposits in the early rift, which is also characterised by the backstepping propagation of the main fault.

5.2.2. Tectonic control in marine environments

In the Middle Miocene, marine transgression occurred through the spreading of the 'Badenian Sea' (Sant et al., 2017). The exact timing of this transition is not defined in the Croatian part of the PBS. According to the dating results, the initial marine flooding events are in the Early to Middle Badenian (Ćorić et al., 2009; Marković, 2017; Brlek et al., 2020). Sequences D-1 and D-2 consist of thick volcanic rocks occasionally interlayered by marine marls in the western part of the study area (Figs. 9 and 4b). The presence of volcanic rocks of Middle Miocene can be correlated with the intense Badenian volcanic activity in the Drava Basin (Pamić et al., 1995), i.e., with the climax of the syn-rift stage (Pavelić, 2001). In the hanging walls of normal faults, a retrogradational stacking pattern was observed in most sequences (Figs. 9 and 11), inferring that the sediment supply rate was lower than the accommodation rate, which is characteristic of the rift climax (Prosser, 1993). The characteristic feature of the entire syn-rift phase was the formation of relatively small but diverse types of extensional structures, from half-grabens to supradetachment basins (Fig. 15). During the late rift stage sequences D and MP developed corresponding to different syn-rift structural units, resulting in a diverse palaeomorphology (Fig. 7b and 13b, and c). Sediments were deposited simultaneously in fan-delta, slope aprons, and shallow to offshore marine environments in relatively small and fragmented basins. We suggest that the reason for this was the formation of multiple syn-rift structures, within a relatively short distance. In addition, two low-angle faults were active, with a possible change in extension accommodated in the transfer zone (relay ramp), while in their hanging wall a number of high-angle faults fragmented the mostly Mesozoic carbonate rocks in the basement.

5.2.2.1. Offshore depositional system in synforms of extensional detachment.
The combination of well data, seismic sections, and attribute maps (Fig. 12b) led to the conclusion that the eastern part of the Krčenik sag and the Noskovci half-graben were represented by basinal sedimentation mixed with basalt and andesite volcanism (Fig. 13b and c). Offshore sedimentation was also confirmed by planktonic foraminifera in these structures and in the depocenters in the eastern part (Fig. 4a and 13b, and c). The location of these main depocenters can be correlated with the sites where changes in the extensional detachment morphology resulted in synform structures (Figs. 6, 9 and 11). The synforms and ridge between them formed in DD and MPD low-angle detachment hanging wall can be compared with structures from other extensional settings (Gibbs, 1983; Withjack and Schlische, 2017; Coleman et al., 2018). Various models have been placed on their formation (McDonnell et al., 2010). We suggest that in the Drava Basin, the inherited structural setting (Balázs et al., 2016), combined with possible differential sedimentary loading, played an important role.

5.2.2.2. Fan-delta controlled by relay ramp.
The relay ramp is a type of transfer zones that develop between normal faults that connect their footwall to the corresponding hanging wall (Athmer and Luthi, 2011).

They are usually zones of transfer of sediments into the depocenters (Young et al., 2000; Commins and Cartwright, 2005; Hemelsdaël and Ford, 2016), but sometimes they can serve as sites of deposition (Giba et al., 2012; Hemelsdaël and Ford, 2016). The interpreted relay ramp is located in the western part od the study area, is gently dipping basin slope between the faults F-1 and DD (Fig. 7). Channel features and amplitude distributions on the attribute map in the D sequence (Fig. 12b) indicate that the main sediment source area was in the foot-wall of the detachment fault system draining into the ramp and Krčenik sag (Fig. 13b and c). The sedimentary infill is characterised by (sub) parallel to discontinuous seismic facies IV with gently dipping reflections (Fig. 9). Subsidence of the sag structure continued from the early to the late rift phase due to extension along the DD fault, providing accommodation space (Fig. 6b) for sediments eroded from the hinterland. The difference between the two rift stages in this area is that deposition was initially controlled by normal F-1 fault and later by the ramp. The ramp served as a depositional area that allowed the progradation of the fan-delta sediments into the sag throughout the late rift stage (Fig. 13 b and c). The relay ramp developed as part of the late rift stage, even though its formation is associated with the onset of fault linkage in the early rift (Athmer and Luthi, 2011). We suggest that this may be the case because of the temporal difference in temporal activity of the two bounding faults. Extension along the DD low-angle detachment enabled subsidence of the ramp in its hanging wall, as well as the formation of the low dip angle of the ramp slope. This allowed the deposition of probably coarse-grained sediments, as shown by the seismic facies observation (Fig. 13b and c).

5.2.2.3. Submarine fan on fault scarp. The fault scarps of the F-31 and MPD faults in the Marjanci graben (Figs. 11 and 15c) were identified as sediment transport zones. The subsidence centres were located near the boundary faults that controlled offshore sedimentation in a large accommodation space, of approximately 10 km wide graben. Sediments from the eroded footwall were deposited directly into the basin as fan-deltas or slope aprons, that appear in the seismic data as wedge-shaped reflections of hummocky to discontinuous seismic facies III (Figs. 4a and 11). The geometry of the seismic facies indicates that the fault-bounded clastic wedges consisted of coarse-grained sediment supplied transversely to the basin. The facies association G with breccias and conglomerates to siltstones, observed in wells intervals within these wedges indicates the variety of gravity flow deposits. Such a succession can be compared to other coarse-grained clastic wedges of the marine syn-rift successions (Wilson et al., 2001; Henstra et al., 2016; Ribes et al., 2019).

5.2.2.4. Fan-delta on tilted fault block. Apart from the fault scarps and structural ramp, the fan-delta deposition was also been interpreted on steep basin slopes. Such fan-deltas were documented on the southern slopes of the Zaláta supradetachment basin and in the western part of the Marjanci graben (Fig. 13b and c). They developed on the dip slopes of eroded tilted fault blocks above the extensional detachment with sedimentation toward the detachment tip (Fig. 15d and f). Seismic data showed steep, downlapping reflectors of seismic facies VI (Fig. 4c). The geometry of the seismic reflectors suggests the formation of a Gilbert-type deep-water delta (Postma, 1988).

6. Conclusions

This study provides insight into the tectonostratigraphic evolution and basin architecture of the syn-rift phase in the Drava Basin, the largest basin in the SW part of the Pannonian Basin System. This study shed light on the influence of inherited structures and detachment geometry on the distribution of the main depocenters. The interpreted extensional detachments are defined as part of the Drava Rift Fault System – the system that enabled the extension, while the rest of the system remains to be investigated. The following conclusions are derived.

- The rifting phase is characterised by the formation of half-graben, graben, sag, and supradetachment basin-type structures, with relay ramp and structural highs
- The entire syn-rift infill was divided into second-order sequences corresponding to two rift stages, early and late. These second-order sequences were further subdivided into third-order sequences corresponding to higher-order tectonic cycles within a syn-rift stage and are the result of local rift migration
- In contrast to the early rift stage, the final rift structures were defined by extension along extensional detachments, which represent the main syn-rift normal fault system in the area. The observed extensional detachments and their metamorphic basements indicate extension of the core-complex-type
- The early rift stage is characterised by continental deposition in alluvial fans, fan deltas, and lacustrine environments. The final rift stage is characterised by marine deposition. Following deposits are determined: shallow-water fan deltas, subaqueous aprons, deep-marine sedimentation, and volcanic activity
- Throughout the syn-rift stage, tectonism was the major factor influencing sediment deposition. The rift climax is characterised by several coeval palaeomorphological features resulting from complex structural relationships between faults. Relay ramp, basin slopes of tilted fault blocks, and fault-scarp were the main sediment transport zones for deposition of alluvial fans, fan deltas, and subaqueous aprons sediments. The main depocenters were within synforms formed by changes in the geometry of extensional detachments and were the main sites of tectonic subsidence.

Credit author statement

David Rukavina: conceptualisation, methodology, investigation, data curation, writing – original draft, review and editing, visualisation. **Bruno Saftić:** conceptualisation, methodology, validation, writing – review and editing, supervision, funding acquisition. **Bojan Matoš:** validation, writing – review and editing, visualisation. **Iva Kolenković Močilac:** formal analysis, writing – review and editing, visualisation. **Vlasta Premec Fuček:** formal analysis, investigation. **Marko Cvetković:** resources, writing – review and editing, supervision, funding acquisition.

Declaration of competing interest

The authors declare that they have no known competing financial interests or personal relationships that could have appeared to influence the work reported in this paper.

Data availability

The authors do not have permission to share data.

References

Allen, P.A., Hovius, N., 1998. Sediment supply from landslide-dominated catchments: implications for basin-margin fans. Basin Res. 10, 19–35. https://doi.org/10.1046/j.1365-2117.1998.00060.x.

Andrić, N., Sant, K., Matenco, L., Mandic, O., Tomljenović, B., Pavelić, D., Hrvatović, H., Demir, V., Ooms, J., 2017. The link between tectonics and sedimentation in asymmetric extensional basins: Inferences from the study of the Sarajevo-Zenica Basin. Mar. Pet. Geol. 83, 305–332. https://doi.org/10.1016/j.marpetgeo.2017.02.024.

Athmer, W., Luthi, S.M., 2011. The effect of relay ramps on sediment routes and deposition : a review. Sediment. Geol. 242, 1–17. https://doi.org/10.1016/j.sedgeo.2011.10.002.

Athmer, W., Uribe, G.A.G., Luthi, S.M., Donselaar, M.E., 2011. Tectonic Control on the Distribution of Palaeocene Marine Syn-Rift Deposits in the Fenris Graben , northwesternVÖring Basin , Offshore Norway 361–375. https://doi.org/10.1111/j.1365-2117.2010.00494.x.

Bada, G., Horváth, F., Dövényi, P., Szafián, P., Windhoffer, G., Cloetingh, S., 2007. Present-day stress field and tectonic inversion in the Pannonian Basin. Glob. Planet. Change 58, 165–180. https://doi.org/10.1016/j.gloplacha.2007.01.007.

Balázs, A., Maţenco, L., Granjeon, D., Alms, K., François, T., Sztanó, O., 2021. Towards stratigraphic-thermo-mechanical numerical modelling: Integrated analysis of asymmetric extensional basins. Glob. Planet. Change 196. https://doi.org/10.1016/j.gloplacha.2020.103386.

Balázs, A., Matenco, L., Magyar, I., Horváth, F., Cloetingh, S., 2016. The link between tectonics and sedimentation in back-arc basins: new genetic constraints from the analysis of the Pannonian Basin. Tectonics 35, 1526–1559. https://doi.org/10.1002/2015TC004109.

Bali, L., Barković, D., Bojanić, I.B., Biro, I., Borozan, D., Dukić, D., Galosi-Kovacs, B., Horvath, F., Kadi, Z., Kitanics, M., Kobor, M., Korokani, B., Musitz, B., Nador, A., Nagymrosy, A., Pap, N., Remenyi, P., Serdarusić, H., Szalayne, E.Sa, Toth, T., Uhrin, A., Unk, J., Vegh, A., Worum, G., 2012. Geothermal Resource Assessment of the Drava Basin. IDResearch Kft./Publikon Publishers.

Brlek, M., Kutterolf, S., Gaynor, S., Kuiper, K., Belak, M., Brčić, V., Holcová, K., Wang, K., Bakrač, K., Hajek-Tadesse, V., Mišur, I., Horvat, M., Šuica, S., Schaltegger, U., 2020. Miocene syn - rift evolution of the North Croatian Basin (Carpathian – Pannonian Region): new constraints from Mts. Kalnik and Požeška gora volcaniclastic record with regional implications. Int. J. Earth Sci. 109, 2775–2800. https://doi.org/10.1007/s00531-020-01927-4.

Brückl, E., Behm, M., Decker, K., Grad, M., Guterch, A., Keller, G.R., Thybo, H., 2010. Crustal structure and active tectonics in the Eastern Alps. Tectonics 29, 1–17. https://doi.org/10.1029/2009tc002491.

Cicha, I., Rögl, F., Rupp, C., Čtyroká, J., 1998. Oligocene – miocene foraminifera of the central Paratethys. Abh. seckenberg. Naturforsch. Ges., Frankfurt a. M. 549, 1–325.

Coleman, A.J., Duffy, O.B., Jackson, C.A.-L., 2018. Growth folds above propagating normal faults. https://doi.org/10.31223/osf.io/naq7h.

Commins, D., Cartwright, J., 2005. Deformed streams reveal growth and linkage of a normal fault array in the Canyonlands graben , Utah. Geology 645–648. https://doi.org/10.1130/G21433.1.

Ćorić, S., Pavelić, D., Rögl, F., Mandic, O., Vrabac, S., Avanić, R., Jerković, L., Vranjkovic, A., 2009. Revised Middle miocene datum for initial marine flooding of north Croatian basins (Pannonian Basin System, central Paratethys). Geol. Croat. 62, 31–43. https://doi.org/10.4154/gc.2013.05.

Csontos, L., Marton, E., Worum, G., Benkovics, L., 2002. Geodynamics of SW-Pannonian inselbergs (Mecsek and villany mts , SW Hungary): inferences from a complex structural analysis. EGU Spec. Publ. Ser. 3, 227–245. https://doi.org/10.5194/smsps-3-227-2002.

Cvetković, M., 2013. Lithostratigraphic Units of the Third Neogene-Quaternary Megacycle in the Sava Depression and Their Petroleum Potential. Faculty of Mining, Geology and Petroleum Engeineering, University of Zagreb, Zagreb, p. 175.

Cvetković, M., Matoš, B., Rukavina, D., Kolenković Močilac, I., Saftić, B., Baketarić, T., Baketarić, M., Vuić, I., Stopar, A., Jarić, A., Paškov, T., 2019. Geoenergy potential of the Croatian part of Pannonian Basin: insights from the reconstruction of the pre-Neogene basement unconformity. J. Maps 15, 651–661. https://doi.org/10.1080/17445647.2019.1645052.

Dolton, G.L., 2006. Pannonian Basin Province, central Europe (Province 4808)—petroleum geology, total petroleum systems, and petroleum resource Assessment. USGS Bull. 2204-B 1–47.

Embry, A.F., 1995. Sequence boundaries and sequence hierarchies: problems and proposals. In: Steel, R.J., Felt, V.L., Johannessen, E.P., Mathieu, C. (Eds.), Sequence Stratigraphy on the Northwest European Margin, Proceedings of the Norwegian Petroleum Society Conference. Norwegian Petroleum Society (NPF), pp. 1–11.

Feng, Y., Jiang, S., Hu, S., Li, S., Lin, C., Xie, X., 2016. Sequence stratigraphy and importance of syndepositional structural slope-break for architecture of Paleogene syn-rift lacustrine strata, Bohai Bay Basin. E. China. Mar. Pet. Geol. 69, 183–204. https://doi.org/10.1016/j.marpetgeo.2015.10.013.

Feng, Z.Z., 2022. Some new thoughts of definitions of terms of sedimentary facies: based on Miall's paper (1985). J. Palaeogeogr. 11, 1–7. https://doi.org/10.1016/j.jop.2022.01.002.

Fodor, L., Balázs, A., Csillag, G., Dunkl, I., Héja, G., Jelen, B., Kelemen, P., Kövér, S., Németh, A., Nyíri, D., Selmeczi, I., Trajanova, M., Vrabec, Marko, Vrabec, Mirijam, 2021. Crustal exhumation and depocenter migration from the Alpine orogenic margin towards the Pannonian extensional back-arc basin controlled by inheritance. Glob. Planet. Change 201. https://doi.org/10.1016/j.gloplacha.2021.103475.

Ford, M., Hemelsdaël, R., Mancini, M., Palyvos, N., 2017. Rift migration and lateral propagation: evolution of normal faults and sediment-routing systems of the western Corinth rift (Greece). Geol. Soc. Spec. Publ. 439, 131–168. https://doi.org/10.1144/SP439.15.

Friedmann, S.J., Burbank, D.W., 1995. Rift basins and supradetachment basins: Intracontinental extensional end-members. Basin Res. 7, 109–127. https://doi.org/10.1111/j.1365-2117.1995.tb00099.x.

Gawthorpe, R.L., Leeder, M.R., 2000. Tectono-sedimentary evolution of active extensional basins. Basin Res. 12, 195–218. https://doi.org/10.1111/j.1365-2117.2000.00121.x.

Giba, M., Walsh, J.J., Nicol, A., 2012. Segmentation and growth of an obliquely reactivated normal fault b Isolated fault model c. J. Struct. Geol. 39, 253–267. https://doi.org/10.1016/j.jsg.2012.01.004.

Gibbs, A., 1987. Development of extension and mixed-mode sedimentary basins. Geol. Soc. Spec. Publ. 28, 19–33. https://doi.org/10.1144/GSL.SP.1987.028.01.03.

Gibbs, A.D., 1983. Journal of Structural Geology. Balanc. Cross-Section Constr. From Seism. Sect. Areas Extensional Tectonics 5.

Grenerczy, G., Sella, G., Stein, S., 2005. Tectonic implications of the GPS velocity field in the northern Adriatic region. Geophys. Res. Lett. 32, 10–13. https://doi.org/10.1029/2005GL022947.

Harzhauser, M., Mandic, O., 2008. Neogene lake systems of Central and South-Eastern Europe: Faunal diversity, gradients and interrelations. Palaeogeogr. Palaeoclimatol. Palaeoecol. 260, 417–434. https://doi.org/10.1016/j.palaeo.2007.12.013.

Hemelsdaël, R., Ford, M., 2016. Relay zone evolution: a history of repeated fault propagation and linkage, central Corinth rift, Greece. Basin Res. 28, 34–56. https://doi.org/10.1111/bre.12101.

Henstra, G.A., Grundvåg, S.-A., Johannessen, E.P., Kristensen, T.B., Midtkandal, I., Nystuen, J.P., Rotevatn, A., Surlyk, F., Sæther, T., Windelstad, J., 2016. Depositional precesses and stratigraphic architecture within a coarse-grained rift-margin turbidite system: the Wollaston Forland Group, east Greenland. Mar. Pet. Geol. https://doi.org/10.1016/j.marpetgeo.2016.05.018.

Hinsken, S., Ustaszewski, K., Wetzel, A., 2007. Graben width controlling syn-rift sedimentation: the Palaeogene southern upper rhine graben as an example. Int. J. Earth Sci. 96, 979–1002. https://doi.org/10.1007/s00531-006-0162-y.

Hohenegger, J., Ćorić, S., Wagreich, M., 2014. Timing of the Middle miocene Badenian stage of the central Paratethys. Geol. Carpathica 65, 55–66. https://doi.org/10.2478/geoca-2014-0004.

Horváth, F., 2012. Towards a dynamic model for the formation of the Pannonian basin. Geophys. Res. Abstr. EGU Gen. Assem. 14, 2012–10178.

Horváth, F., 1995. Phases of compression during the evolution of Pannonian Basin and its bearing on hydrocharbon exploration. Mar. Pet. Geol. 12, 837–844.

Horváth, F., Bada, G., Szafián, P., Tari, G., Ádám, A., Cloetingh, S., 2006. Formation and deformation of the Pannonian Basin: constraints from observational data. Geol. Soc. London, Mem. 32, 191–206. https://doi.org/10.1144/GSL.MEM.2006.032.01.11.

Hou, Y., He, S., Ni, J., Wang, B., 2012. Tectono-sequence stratigraphic analysis on Paleogene Shahejie formation in the Banqiao sub-basin, eastern China. Mar. Pet. Geol. 36, 100–117. https://doi.org/10.1016/j.marpetgeo.2012.06.001.

Huismans, R.S., Podladchikov, Y., Cloetingh, S., 2001. Dynamic modeling of the transition from passive to active rifting, application to the Pannonian Basin. Tectonics 20, 1021–1039. https://doi.org/10.1029/2001TC900010.

Jamičić, D., 1995. The role of sinistral strike-slip faults in the formation of the structural Fabric of the Slavonian Mts. (eastern Croatia). Geol. Croat. 48, 155–160. https://doi.org/10.4154/GC.1995.12.

Jia, L., Zhong, D., Ji, Y., Zhou, Y., Liu, J., Mi, L., Li, D., Yan, R., Yi, Z., Jia, L., 2019. Architecture of tectonic sequences, depositional systems, and tectonic controls of the sedimentary fills of the rift-related Wenchang Formation in the Lufeng Depression, Pearl River Mouth Basin, China. Geol. J. 54, 1950–1975. https://doi.org/10.1002/gj.3272.

Khalil, S.M., Mcclay, K.R., 2009. Structural control on syn-rift sedimentation , northwestern Red Sea margin , Egypt. Mar. Pet. Geol. 26, 1018–1034. https://doi.org/10.1016/j.marpetgeo.2008.09.001.

Leppard, C.W., Gawthorpe, R.L., 2006. Sedimentology of rift climax deep water systems; lower Rudeis formation, Hammam Faraun fault block, Suez rift, Egypt. Sediment. Geol. 191, 67–87. https://doi.org/10.1016/j.sedgeo.2006.01.006.

Lister, G.S., Davis, G.A., 1989. The origin of metamorphic core complexes and detachment faults formed during Tertiary continental margins. Geology 14, 65–94. https://doi.org/10.1016/0191-8141(89)90036-9.

Lučić, D., Saftić, B., Krizmanić, K., Prelogović, E., Britvić, V., Mesić, I., Tadej, J., 2001. The Neogene evolution and hydrocarbon potential of the Pannonian Basin in Croatia. Mar. Pet. Geol. 18, 133–147. https://doi.org/10.1016/S0264-8172(00)00038-6.

Magyar, I., Geary, D.H., Müller, P., 1999. Paleogeographic evolution of the late miocene Lake Pannon in central Europe. Palaeogeogr. Palaeoclimatol. Palaeoecol. 147, 151–167. https://doi.org/10.1016/S0031-0182(98)00155-2.

Mandić, O., de Leeuw, A., Bulić, J., Kuiper, K.F., Krijgsman, W., Jurišić-Polšak, Z., 2012. Paleogeographic evolution of the southern Pannonian Basin:40Ar/39Ar age constraints on the miocene continental series of northern Croatia. Int. J. Earth Sci. 101, 1033–1046. https://doi.org/10.1007/s00531-011-0695-6.

Mandić, O., Kurečić, T., Neubauer, T.A., Harzhauser, M., 2015. Stratigraphic and paleogeographic significance of lacustrine mollusks from the Pliocene Viviparus beds in central Croatia. Geol. Croat. 68, 179–207. https://doi.org/10.4154/GC.2015.15.

Marković, F., 2017. Miocene Tuffs from the North Croatian Basin. Faculty of Science, Department of Geology, University of Zagreb, Zagreb, p. 174.

Matenco, L.C., Haq, B.U., 2020. Multi-scale depositional successions in tectonic settings. Earth-Science Rev. 200, 102991 https://doi.org/10.1016/j.earscirev.2019.102991.

Matoš, B., 2014. Neotectonic and Recently Active Faults in Bilogora Mountain Area and Assessment of Their Seismogenic Potential. Faculty of Mining Geology and Petroleum Engineering, Universty of Zagreb, Zagreb, p. 256.

Matoš, B., Pérez-Peña, J.V., Tomljenović, B., 2016. Landscape response to recent tectonic deformation in the SW Pannonian Basin: evidence from DEM-based morphometric analysis of the Bilogora Mt. area, NE Croatia. Geomorphology 263, 132–155. https://doi.org/10.1016/j.geomorph.2016.03.020.

McDonnell, A., Jackson, M.P.A., Hudec, M.R., 2010. Origin of transverse folds in an extensional growth-fault setting: evidence from an extensive seismic volume in the western Gulf of Mexico. Mar. Pet. Geol. 27, 1494–1507. https://doi.org/10.1016/j.marpetgeo.2010.03.006.

Milia, A., Torrente, M.M., 2015. Rift and supradetachment basins during extension: insight from the Tyrrhenian rift. J. Geol. Soc. London. 172, 5–8. https://doi.org/10.1144/jgs2014-046.

Morley, C.K., 1990. Transfer zones in the East African Rift System and their relevance to hydrocarbon exploration in rifts. Am. Assoc. Pet. Geol. Bull. 74, 1234–1253.

Morley, C.K., Nelson, R.A., Patton, T.L., Munn, S.G., 1990. Transfer zones in the East African rift system and their relevance to hydrocarbon exploration in rifts. Am. Assoc. Pet. Geol. Bull. https://doi.org/10.1306/0c9b2475-1710-11d7-8645000102c1865d.

Müller, B., Zoback, M.L., Fuchs, K., Mastin, L., Gregersen, S., Pavoni, N., Stephansson, O., Ljunggren, C., 1992. Regional patterns of tectonic stress in Europe. J. Geophys. Res. 97, 11.

Muravchik, M., Henstra, G.A., Eliassen, G.T., Gawthorpe, R.L., Leeder, M., Kranis, H., Skourtsos, E., Andrews, J., 2020. Deep-water sediment transport patterns and basin floor topography in early rift basins : Plio-Pleistocene syn-rift of the Corinth Rift , Greece. Basin Res. 1184–1212. https://doi.org/10.1111/bre.12423.

Pamić, J.J., McKee, E.H., Bullen, T.D., Lanphere, M.A., 1995. Tertiary volcanic rocks from the southern Pannonian Basin, Croatia. Int. Geol. Rev. 37, 259–283. https://doi.org/10.1080/00206819509465404.

Pavelić, D., 2001. Tectonostratigraphic model for the North Croatian and north Bosnian sector of the miocene Pannonian Basin System. Basin Res. 13, 359–376. https://doi.org/10.1046/j.0950-091X.2001.00155.x.

Pavelić, D., 1987. Litološke osobine Mosti-člana duboke bušotine Ševkovica-11 (Istočna Hrvatska). Nafta 38, 541–545.

Pavelić, D., Kovačić, M., 2018. Sedimentology and stratigraphy of the Neogene rift-type north Croatian basin (Pannonian Basin System, Croatia): a review. Mar. Pet. Geol. 91, 455–469. https://doi.org/10.1016/j.marpetgeo.2018.01.026.

Pavelić, D., Kovačić, M., 1999. Lower miocene alluvial deposits of the Požeška Mt. (Pannonian Basin, northern Croatia): cycles, Megacycles and tectonic implications. Geol. Croat. 52, 67–76. https://doi.org/10.4154/gc.2013.05.

Pavelić, D., Miknic, M., Sarkotić Šrlat, M., 1998. Early to Middle Miocene facies succession in lacustrine and marine environments on the southwestern margin of the Pannonian Basin System (Croatia). Geol. Carpathica 433–443.

Peacock, D.C.P., Knipe, R.J., Sanderson, D.J., 2000. Glossary of normal faults. J. Struct. Geol. 22, 291–305. https://doi.org/10.1016/S0191-8141(00)80102-9.

Pérez-Gussinyé, M., Andrés-Martínez, M., Araújo, M., Xin, Y., Armitage, J., Morgan, J.P., 2020. Lithospheric strength and rift migration controls on Synrift stratigraphy and Breakup unconformities at rifted margins: Examples from numerical models, the Atlantic and south China sea margins. Tectonics 39, 1–37. https://doi.org/10.1029/2020TC006255.

Piller, W.E., Harzhauser, M., Mandic, O., 2007. Miocene Central Paratethys stratigraphy – current status and future directions. Stratigraphy 4, 151–168.

Postma, G., 1988. Depositional architecture and facies of river and fan deltas: a synthesis. Assoc. Sedimentol. Spec. Publ. 16, 9–15. https://doi.org/10.1002/0264-8172(93)90023-l.

Prelogović, E., Saftić, B., Kuk, V., Velić, J., Dragaš, M., Lučić, D., 1998. Tectonic activity in the Croatian part of the Pannonian basin. Tectonophysics 297, 283–293. https://doi.org/10.1016/S0040-1951(98)00173-5.

Prosser, S., 1993. Rift-related linked depositional systems and their seismic expression. Geol. Soc. London, Spec. Publ. 71, 35–66. https://doi.org/10.1144/GSL.SP.1993.071.01.03.

Ratschbacher, L., Merle, O., Davy, P., Cobbold, P., 1991. Lateral extrusion in the eastern Alps, Part 1: boundary conditions and experiments scaled for gravity. Tectonics 10, 245–256. https://doi.org/10.1029/90TC02622.

Ravnås, R., Steel, R.J., 1998. Architecture of marine rift-basin successions. Am. Assoc. Pet. Geol. Bull. 82, 110–146. https://doi.org/10.1306/1D9BC3A9-172D-11D7-8645000102C1865D.

Ribes, C., Ghienne, J., Manatschal, G., Decarlis, A., Karner, G.D., Figueredo, P.H., Johnson, C.A., 2019. Long-lived Mega Fault-Scarps and Related Breccias at Distal Rifted Margins : Insights from Present-Day and Fossil Analogues, vol. 176, pp. 801–816.

Richards, M., Bowman, M., 1998. Submarine fans and related depositional systems II: variability in reservoir architecture and wireline log character. Mar. Pet. Geol. 15, 821–839. https://doi.org/10.1016/S0264-8172(98)00042-7.

Ritts, B.D., Berry, A.K., Johnson, C.L., Darby, B.J., Davis, G.A., 2010. Early Cretaceous supradetachment basins in the Hohhot metamorphic core complex, Inner Mongolia, China. Basin Res. 22, 45–60. https://doi.org/10.1111/j.1365-2117.2009.00433.x.

Rosendahl, B.R., 1987. Architecture of continental rifts with special reference to east africa. Annu. Rev. Earth Planet Sci. 15, 445–503.

Royden, L., Horváth, F., János, R., 1983a. Evolution of Pannonian Basin System 1. Tectonics. Tectonics 2, 63–90.

Royden, L., Horváth, F., Nagymarosy, A., Steaena, L., 1983b. Evolution of the Pannonian Basin System 2. Subsidence and thermal history. Tectonics 2, 91–137.

Royden, L.H., 1993. Evolution of retreating subduction boundaries formed. During Continental Collision 12, 629–638.

Saftić, B., Velić, J., Sztano, O., Juhasz, G., Ivković, Ž., 2003. Tertiary subsurface facies, source rocks and hydrocarbon reservoirs in the SW part of the Pannonian Basin (northern Croatia and south-western Hungary). Geol. Croat. 56, 101–122.

Sant, K., Palcu, V., , D., Mandic, O., Krijgsman, W., 2017. Changing seas in the early–Middle miocene of central Europe: a Mediterranean approach to Paratethyan stratigraphy. Terra Nov 29, 273–281. https://doi.org/10.1111/ter.12273.

Santos, M.G.M., Almeida, R.P., Godinho, L.P.S., Marconato, A., Mountney, N.P., 2014. Distinct styles of fluvial deposition in a Cambrian rift basin. Sedimentology 61, 881–914. https://doi.org/10.1111/sed.12074.

Schmid, S.M., Bernoulli, D., Fügenschuh, B., Matenco, L., Schefer, S., Schuster, R., Tischler, M., Ustaszewski, K., 2008. The Alpine-Carpathian-Dinaridic orogenic system: correlation and evolution of tectonic units. Swiss J. Geosci. 101, 139–183. https://doi.org/10.1007/s00015-008-1247-3.

Sebe, K., Kovačić, M., Magyar, I., Krizmanić, K., Špelić, M., Bigunac, D., Sütő-Szentai, M., Kovács Szuromi-Korecz, A., Bakrač, K., Hajek-Tadesse, V., Troskot-Čorbić, T., Sztanó, A., 2020. Correlation of upper miocene-pliocene lake pannon deposits across the Drava basin, Croatia and Hungary. Geol. Croat. 73, 177–195. https://doi.org/10.4154/gc.2020.12.

Šimon, J., 1973. O nekim rezultatima regionalne korelacije litostratigrafskih jedinica u jugozapadnom području Panonskog bazena. Nafta 24/12, 623–630.

Sremac, J., Vrsaljko, D., Karaica, B., Tripalo, K., Firi, K.F., Marjanac, T., 2016. Reefs and bioaccumulations in the Miocene deposits of the North Croatian Basin – Amazing diversity yet to be described. Mining-Geology-Petroleum Eng. Bull. 31, 19–30. https://doi.org/10.17794/rgn.2016.1.2.

Stojadinović, U., Matenco, L., Andriessen, P.A.M., Toljić, M., Foeken, J.P.T., 2013. The balance between orogenic building and subsequent extension during the tertiary evolution of the NE Dinarides: constraints from low-temperature thermochronology. Glob. Planet. Change 103, 19–38. https://doi.org/10.1016/j.gloplacha.2012.08.004.

Tan, C., Yu, X., Liu, B., Qu, J., Zhang, L., Huang, D., 2017. Conglomerate categories in coarse-grained deltas and their controls on hydrocarbon reservoir distribution: a case study of the Triassic Baikouquan Formation, Mahu Depression, NW China. Pet. Geosci. 23, 403–414. https://doi.org/10.1144/petgeo2016-017.

Tari, G., Horváth, F., Rumpler, J., 1992. Styles of extension in the Pannonian Basin. Tectonophysics 208, 203–219. https://doi.org/10.1016/0040-1951(92)90345-7.

Tišljar, J., 1993. Sedimentary bodies and depositional models for the Miocene oil-producing areas of Ladislavci, Beničanci and Obod. Nafta 44, 531–542.

Tomljenović, B., Csontos, L., 2001. Neogene-quaternary structures in the border zone between Alps, Dinarides and Pannonian Basin (Hrvatsko zgorje and Karlovac basins, Croatia). Int. J. Earth Sci. 90, 560–578. https://doi.org/10.1007/s005310000176.

Ustaszewski, K., Herak, M., Tomljenović, B., Herak, D., Matej, S., 2014a. Neotectonics of the Dinarides-Pannonian Basin transition and possible earthquake sources in the Banja Luka epicentral area. J. Geodyn. 82, 52–68. https://doi.org/10.1016/j.jog.2014.04.006.

Ustaszewski, K., Herak, M., Tomljenović, B., Herak, D., Matej, S., 2014b. Neotectonics of the Dinarides-Pannonian Basin transition and possible earthquake sources in the Banja Luka epicentral area. J. Geodyn. 82, 52–68. https://doi.org/10.1016/j.jog.2014.04.006.

Ustaszewski, K., Kounov, A., Schmid, S.M., Schaltegger, U., Krenn, E., Frank, W., Fügenschuh, B., 2010. Evolution of the Adria-Europe plate boundary in the northern Dinarides: from continent-continent collision to back-arc extension. Tectonics 29, 34. https://doi.org/10.1029/2010TC002668.

Velić, J., Malvić, T., Cvetković, M., 2011. Palinspastic reconstruction of synsedimentary tectonics of Neogene and quaternary sediments in the kloštar field (Sava depression, Pannonian Basin, Croatia). Zeitschrift der Dtsch. Gesellschaft fur Geowissenschaften 162, 193–201. https://doi.org/10.1127/1860-1804/2011/0162-0193.

Vrsaljko, D., Pavelić, D., Bajraktarević, Z., 2005. Stratigraphy and palaeogeography of miocene deposits from the marginal area of Žumberak Mt. And the samoborsko gorje Mts. (northwestern Croatia). Geol. Croat. 58, 133–150. https://doi.org/10.4154/GC.2005.07.

Vrsaljko, D., Pavelić, D., Miknić, M., Brkić, M., Kovačić, M., Hećimović, I., Hajek-Tadesse, V., Avanić, R., Kurtanjek, N., 2006. Middle miocene (upper Badenian/Sarmatian) Palaeoecology and evolution of the environments in the area of medvednica Mt. (North Croatia). Geol. Croat. 59, 51–63. https://doi.org/10.4154/GC.2006.04.

Wilson, R.C.L., Manatschal, G., Wise, S., 2001. Rifting along non-volcanic passive margins : stratigraphic and seismic evidence from the Mesozoic successions of the Alps and western Iberia. In: Non-Volcanic Rifting of Continental Margina: A Comparison of Evidence from Land and Sea, pp. 429–452.

Windhoffer, G., Bada, G., Nieuwland, D., Wórum, G., Horváth, F., Cloetingh, S., 2005. On the mechanics of basin formation in the Pannonian basin: Inferences from analogue and numerical modelling. Tectonophysics 410, 389–415. https://doi.org/10.1016/j.tecto.2004.10.019.

Withjack, M.O., Schliche, R.W., Olsen, P.E., 2002. Rift-basin structure and its influence on sedimentary systems. SEPM Spec. Publ. Sediment. Cont. Rift. 57–81. https://doi.org/10.2110/pec.02.73.0057.

Withjack, M.O., Schlische, R.W., 2017. Geometric and experimental models of extensional fault-bend folds. Geol. Soc. London, Spec. Publ. 253, 285–305.

Wu, H., Ji, Y., Wu, C., Duclaux, G., Wu, H., Gao, C., Li, L., Chang, L., 2019. Stratigraphic response to spatiotemporally varying tectonic forcing in rifted continental basin: insight from a coupled tectonic-stratigraphic numerical model. Basin Res. 31, 311–336. https://doi.org/10.1111/bre.12322.

Young, M.J., Gawthorpe, R.O.B.L., Sharp, I.A.N.R., 2000. Sedimentology and Sequence Stratigraphy of a Transfer Zone Coarse-Grained Delta , Miocene Suez Rift , Egypt.

Zečević, M., Velić, J., Sremac, J., Troskot-Čorbić, T., Garašić, V., 2010. Significance of the Badenian petroleum source rocks from the Krndija Mt. (Pannonian Basin, Croatia). Geol. Croat. 63, 225–239, 104154/gc.2010.19.

Zhu, H., Yang, X., Liu, K., Zhou, X., 2014. Seismic-based sediment provenance analysis in continental lacustrine rift basins: an example from the Bohai Bay Basin, China. Am. Assoc. Pet. Geol. Bull. 98, 1995–2018. https://doi.org/10.1306/05081412159.